

# 000 001 002 UNICA: UNIFIED COVARIATE ADAPTATION FOR TIME 003 SERIES FOUNDATION MODEL 004 005 006

007 **Anonymous authors**  
008 Paper under double-blind review  
009  
010  
011

## ABSTRACT

013 Time Series Foundation Models (TSFMs) have achieved remarkable success  
014 through large-scale pretraining. However, their design primarily targets real-  
015 valued series, limiting their ability to handle general forecasting tasks involving di-  
016 verse and often *heterogeneous covariates*—such as categorical variables and mul-  
017 timodal data (e.g., images, text)—which are typically task-specific and difficult  
018 to leverage during pretraining. To address this gap, we propose Unified Covariate  
019 Adaptation (UniCA), a framework to bridge TSFMs with general covariate-aware  
020 forecasting. UniCA first performs covariate homogenization to transform hetero-  
021 geneous covariates into high-level homogeneous series representations and then  
022 fuses them via a unified attention-based fusion mechanism. UniCA is compatible  
023 and universal for adaptation with both homogeneous and heterogeneous covari-  
024 ates, incorporating extra covariate information while preserving the generalization  
025 ability of TSFMs. Extensive experiments on multiple unimodal and multimodal  
026 covariate-aware forecasting benchmarks demonstrate the superiority of UniCA,  
027 highlighting the promise of covariate-aware TSFM adaptation in real-world fore-  
028 casting scenarios. Code: <https://anonymous.4open.science/r/UniCA-C5E0>.  
029  
030

## 1 INTRODUCTION

031 Time series forecasting is essential in a wide  
032 range of domains, including environmental  
033 monitoring Gruca et al. (2022), traffic man-  
034 agement Kadiyala & Kumar (2014), energy  
035 systems Kardakos et al. (2013), communica-  
036 tion networks Peng et al. (2013), and health-  
037 care Morid et al. (2023). Accurate forecasting  
038 supports critical decisions in planning, policy-  
039 making, and operations. Traditional statisti-  
040 cal models such as ARIMA and Exponential  
041 Smoothing Box et al. (2015) have been widely  
042 used for their simplicity and effectiveness in  
043 specific settings. With the advancement of deep  
044 learning, models based on Recurrent Neural  
045 Networks (RNNs) Hochreiter & Schmidhuber  
046 (1997); Cho et al. (2014); Rangapuram et al. (2018) and Convolutional Neural Networks (CNNs) Bai  
047 et al. (2018); Franceschi et al. (2019) have enabled more expressive modeling of complex temporal  
048 dynamics. Transformer-based architectures Zhou et al. (2021); Nie et al. (2023); Liu et al. (2024b)  
049 further advanced the field by capturing long-range dependencies and achieving strong performance,  
050 particularly in long-horizon multivariate forecasting. Inspired by the success of foundation models  
051 in NLP and vision Devlin et al. (2019); Brown et al. (2020); Radford et al. (2021); Kirillov et al.  
052 (2023), recent Time Series Foundation Models (TSFMs) Das et al. (2024); Woo et al. (2024); Ansari  
053 et al. (2024); Goswami et al. (2024) have shown strong generalization capability by pretraining  
on large-scale time series. They learn transferable temporal representations and deliver impressive  
performance even in zero-shot scenarios.

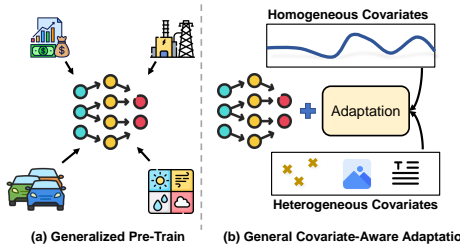


Figure 1: TSFMs are pretrained on time series from diverse domains. However, many tasks contain homo/heterogeneous covariates that are hard to use in pre-training. Adaptation methods to handle these covariates are important in these tasks.

1

054 However, most state-of-the-art TSFMs (Ansari et al., 2024; Das et al., 2024; Goswami et al., 2024)  
 055 are fundamentally designed for univariate forecasting, processing each time series in isolation. This  
 056 architectural choice renders them unable to leverage the critical relationships between a target se-  
 057 ries and its exogenous covariates, limiting their applicability in many real-world scenarios. Some  
 058 TSFMs adopt covariate-aware (Woo et al., 2024) strategies during pretraining; yet, models trained  
 059 in this manner often fail to achieve stable and superior performance across diverse tasks (Aksu et al.,  
 060 2024). More fundamentally, the standard TSFM pretraining paradigm imposes a key limitation: it  
 061 can only effectively leverage homogeneous covariates (e.g., real-valued time series similar to the tar-  
 062 get variable). This restricts their ability to handle heterogeneous covariates, which are increasingly  
 063 common in practical scenarios. Heterogeneous covariates typically includes structured categorical  
 064 variables (e.g., item IDs, calendar features) and multimodal inputs (e.g., images, texts) (Ma et al.,  
 065 2024; Liu et al., 2024a). The diversity and task-specific nature make their integration into existing  
 066 TSFM pipelines non-trivial.

067 While prior work has addressed unimodal covariate-aware forecasting or multi-modal forecasting  
 068 through specialized model architectures Salinas et al. (2020); Lim et al. (2019); Das et al. (2023);  
 069 Jin et al. (2024); Ma et al. (2024); Liu et al. (2024a), these methods are often biased to the task-  
 070 specific data, lack the generalization ability, and underperform compared to large-scale pretrained  
 071 TSFM models (Aksu et al., 2024). Therefore, a key challenge remains: *How can we adapt powerful*  
 072 *pretrained TSFMs to general covariate-aware forecasting, including homogeneous and heteroge-*  
 073 *neous covariates, without losing the generalization ability obtained from pretraining?*

074 In this paper, we address this challenge by proposing a unified and effective adaptation method  
 075 named **Unified Covariate Adaptation (UniCA)**. The core idea is to perform *covariate homoge-*  
 076 *nization* that transforms heterogeneous covariates into a unified, homogeneous temporal representa-  
 077 tion, representing the high-level feature changing over time. This transformation allows us to solve  
 078 the general covariate forecasting with a unified framework in the time series modality. In addition,  
 079 we design an attention-based fusion mechanism with pre-fusion and post-fusion components that  
 080 incorporate covariate information before and after the TSFM backbone, respectively, with the  
 081 parameters of the TSFMs unchanged. The adaptation modules fully utilize the encoding and temporal  
 082 extraction power of the TSFMs, incorporating the covariates' information while retaining the fore-  
 083 casting ability obtained during their pretraining process. Extensive experiments across a wide range  
 084 of benchmarks, including traditional single-modal covariate datasets and challenging multimodal  
 085 datasets, demonstrate the effectiveness and flexibility of UniCA. Our results show that by properly  
 086 adapting covariate information into the series space, TSFMs can significantly outperform specialized  
 087 models, thus opening new possibilities for general-purpose time series forecasting in covariate-rich  
 088 environments. Our main contributions are summarized as follows:

- 089 • We formalize the problem of adapting Time Series Foundation Models (TSFMs) to general  
 090 covariate-aware forecasting scenarios, where the heterogeneous covariates, like categorical or  
 091 multi-modal covariates, can not be directly utilized by TSFMs.
- 092 • We propose Unified Covariate Adaptation (UniCA), a novel framework featuring: (a) *covariate*  
 093 *homogenization* to transform diverse covariates into a unified temporal representation, and (b) a  
 094 dual attention-based fusion mechanism to integrate covariate representation with a frozen TSFM  
 095 backbone.
- 096 • We conduct comprehensive experiments across single-modal and multimodal covariate datasets,  
 097 demonstrating that UniCA enables TSFMs to achieve superior performance compared to task-  
 098 specific baselines. The effectiveness of covariate homogenization on TSFMs and specialized  
 099 methods also proves that it is a simple way to integrate heterogeneous covariates.

## 100 2 RELATED WORK

101 **Time Series Foundation Models (TSFMs).** Recent efforts (Ansari et al., 2024; Woo et al.,  
 102 2024; Goswami et al., 2024; Das et al., 2024; Ekambaram et al., 2024) have developed large-  
 103 scale pretrained models for time series, enabling zero-shot forecasting or fine-tuning across tasks.  
 104 Moirai (Woo et al., 2024), MOMENT (Goswami et al., 2024), and TimesFM (Das et al., 2024)  
 105 adopt a patch-based transformer architecture, while TTM (Ekambaram et al., 2024) builds on  
 106 TSMixer (Ekambaram et al., 2023), which uses MLPs to mix temporal and feature dimensions.  
 107 In contrast, Chronos (Ansari et al., 2024) tokenizes time series into discrete vocabularies and

108 trains language models directly on these sequences. TSFMs are trained based on either channel-  
 109 independence (Han et al., 2024; Goswami et al., 2024; Das et al., 2024; Ansari et al., 2024) that  
 110 ignores covariates, or the equivariant attention mechanism (Woo et al., 2024) that requires covariates  
 111 to be homogeneous. The adaptation to heterogeneous covariates scenarios is an unsolved challenge.  
 112

113 **Forecasting with Covariates.** Covariates play a crucial role in capturing external signals in fore-  
 114 casting tasks. Classical models like ARIMA (Box & Jenkins, 1968) incorporate them via extra co-  
 115 efficients, while deep models such as DeepAR (Salinas et al., 2020) and TFT (Lim et al., 2019) inte-  
 116 grate them as inputs or through specialized encoders. NBEATSx (Olivares et al., 2021) concatenates  
 117 covariates with the main series for fixed-size input. TTM-CM (Ekambaram et al., 2024) introduces  
 118 a fine-tuning approach based on channel mixing. (Chen & Zhao, 2024) introduces MiTSformer to  
 119 handle mixed time series by recovering latent continuous representations from discrete variables to  
 120 mitigate heterogeneity. Among TSFMs, only Moirai (Woo et al., 2024) natively supports covariates  
 121 by flattening series and covariates into a joint sequence, using variate IDs for differentiation. None  
 122 of the existing methods can handle both homogeneous and heterogeneous, especially multi-modal  
 123 covariates, while our method is meant to solve this challenge.

124 **Multimodal Time Series Forecasting.** Most multimodal forecasting studies focus on textual en-  
 125 hancement. A line of work seeks to utilize the powerful temporal encoding ability of LLM to im-  
 126 prove the forecaster (Zhou et al., 2023; Gruver et al., 2023). While these methods provide the pos-  
 127 sibility for multimodal forecasting, they usually handle static textual data. Another line combines  
 128 numerical time series with dynamic textual data, *e.g.* news (Dheenadayalan et al., 2022; Wang et al.,  
 129 2024a) or weather reports (Obst et al., 2019). Time-MMD (Liu et al., 2024a) introduces a multimodal  
 130 dataset and a model that processes time and text modalities independently and merges them via lin-  
 131 ear fusion. Towards image covariates, FusionSF (Ma et al., 2024) proposed the MMSP dataset and a  
 132 method meant especially for the satellite scenario. Our approach proposed a new way that converts  
 133 information from other modalities into series and handles them uniformly in time series modality.

134 **Adapting TSFMs to handle Covariates.** Standard foundation model adaptation, often employ-  
 135 ing parameter-efficient methods like adapters (Houlsby et al., 2019) and LoRA (Hu et al., 2022),  
 136 typically assumes consistency between pretraining and downstream task input/output structures.  
 137 Adapting TSFMs to handle covariates is more complex. While methods like TimesFM (Das et al.,  
 138 2024), which uses an auxiliary regressor for residual correction, and ChronosX (Pineda-Arango  
 139 et al., 2025), which injects covariates through linear transformations but limits its application to  
 140 only point-wise TSFM. All the current adaptation methods struggle with heterogeneous covariates,  
 141 highlighting the need for more flexible adaptation strategies, which our proposed method provides.

### 3 PROBLEM FORMULATION

144 **General Covariates-Aware Time Series Forecasting.** In covariates-aware time series forecast-  
 145 ing, the objective is to predict  $\mathbf{Y}_{T+1:T+H} \in \mathbb{R}^{H \times 1}$  by utilizing both past observations of the target  
 146  $\mathbf{Y}_{1:T} \in \mathbb{R}^{T \times 1}$  and the external covariates, as well as considering their temporal relationships. The  
 147 model takes into account both static covariates  $\mathbf{S}$  and dynamic covariates  $\mathbf{C}_{1:T+H}$ <sup>1</sup> to make predic-  
 148 tions about the future. Formally, we can express the prediction problem as:

$$\hat{\mathbf{Y}}_{T+1:T+H} = f(\mathbf{Y}_{1:T}, \mathbf{C}_{1:T+H}, \mathbf{S}),$$

149 where the static covariates  $\mathbf{S}$  remain unchanged within a series. The dynamic covariates  $\mathbf{C}_{1:T+H}$   
 150 may provide extra information about the past or future state. Both  $\mathbf{S}$  and  $\mathbf{C}_{1:T+H}$  may contain  
 151 *homogeneous* and *heterogeneous* covariates.

152 **Heterogeneous Covariates.** In traditional time series analysis tasks, exogenous covariates typi-  
 153 cally share the same form as the target series, often represented as real-valued numerical variables.  
 154 This homogeneity allows exogenous covariates and targets to be processed under a unified model-  
 155 ing framework without the need for modality-specific designs (Woo et al., 2024; Liu et al., 2024b).  
 156 Such covariates are referred to as *homogeneous covariates*. However, with the advancement of data  
 157 collection, covariates in modern forecasting scenarios exhibit increasingly diverse forms. In many  
 158 practical applications, covariates are no longer restricted to simple real-valued signals but may in-  
 159 volve a wide range of data types. Among these, a particularly significant challenge for TSFMs

160 <sup>1</sup>For notational simplicity, we denote both future-known and future-unknown covariates as  $\mathbf{C}_{1:T+H}$ . For  
 161 future-unknown covariates, the values in the interval  $[T + 1 : T + H]$  are unobserved at prediction time  $T$ .

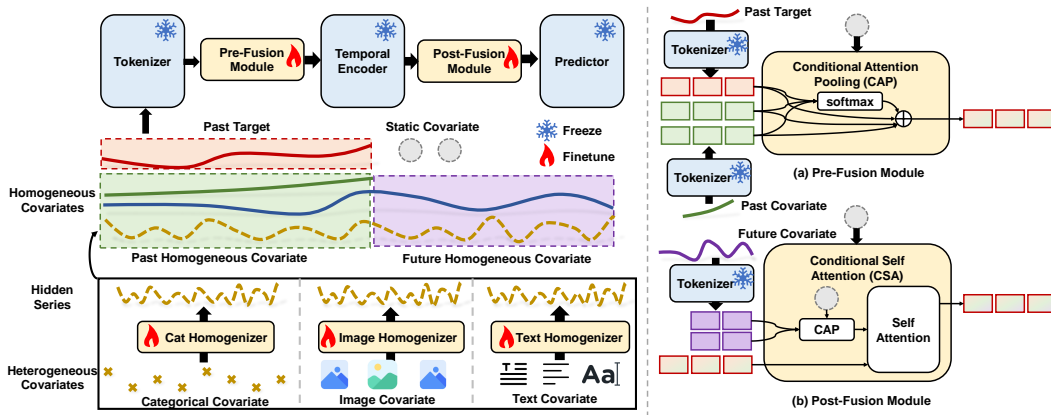


Figure 2: Overview of **Unified Covariate Adapter (UniCA)**. UniCA consists of two key pipelines (1) **Covariate Homogenization**: We use a converter to transform heterogeneous covariates into dense continuous series representations, thus reducing the heterogeneity gap between covariates and target time series. (2) **Modular Fusion**: We decompose the TSFM architecture into interpretable stages and insert Pre-Fusion and Post-Fusion modules to inject covariate information at appropriate locations without interfering with the model’s pretrained dynamics.

comes from *heterogeneous covariates*. These covariates can be broadly categorized into two major types: (1) **Categorical covariates**: Discrete attributes such as item identifiers, store locations, event types, or temporal markers. These variables are not inherently numerical and require embedding techniques or specialized handling to be incorporated into forecasting models. (2) **Multimodal covariates**: High-dimensional, complex data modalities such as images, text descriptions. The emergence of heterogeneous covariates poses fundamental challenges to existing TSFM architectures. Unlike homogeneous covariates, which can be directly integrated, heterogeneous covariates demand modality-specific preprocessing, feature extraction, and fusion strategies.

**Covariate-Aware Adaptation.** Time Series Foundation Models (TSFMs) are designed to model the temporal dependencies within a given series. These models are trained on diverse time series from different domains, which makes it hard to incorporate covariates across different domains. *covariate adaptation* involves modifying the model architecture to integrate the covariate information while fully utilizing the temporal encoding ability. The mathematical formulation of this task can be expressed as follows: Given a TSFM  $f_{fm}$ , the objective is to construct a new forecaster based on the trained foundation model:

$$\tilde{Y}_{T+1:T+H} = g_{ada} \circ f_{fm}(\mathbf{Y}_{1:T}, \mathbf{C}_{1:T+H}, \mathbf{S}), \quad (1)$$

where  $g_{ada}$  is the adaptation module, and  $g_{ada} \circ f_{fm}$  is the composition model after adaptation. In contrast to training covariate-aware deep learning models from scratch, covariate adaptation involves three distinct challenges:

- **Compatibility**: The adaptation module should be compatible with pretrained TSFMs without requiring extensive full-model retraining or architecture redesign.
- **Universality**: It should be able to handle both homogeneous and heterogeneous covariates.
- **Generalization Preservation**: It should leverage the temporal encoding capabilities learned during pretraining while preserving the generalization ability of the foundation model.

In response to these challenges, we propose **Unified Covariate Adaptation (UniCA)**.

## 4 METHODOLOGY

**Unified Covariate Adaptation (UniCA)** is a general framework that enables Time Series Foundation Models (TSFMs) to effectively incorporate heterogeneous covariate information without disrupting their pretrained temporal modeling capabilities. At a high level, UniCA follows two key principles (1) **Covariate Homogenization**: We transform categorical and multimodal covariates into dense continuous series representations, thus reducing the heterogeneity gap between covariates and

target time series. (2) **Modular Fusion**: We decompose the TSFM architecture into interpretable stages and insert an attention-based fusion module to inject covariate information at appropriate locations without interfering with the model’s pretrained dynamics.

#### 4.1 COVARIATE HOMOGENIZATION

To address covariate heterogeneity, UniCA introduces a homogenization process that converts all covariates into a unified homogeneous space. Specifically, categorical covariates are processed using embedding layers that map discrete tokens into continuous vectors. Multimodal covariates—such as images or texts—are initially fed through modality-specific encoders (e.g., convolutional neural networks for images, pretrained transformers for text) to obtain dense feature representations  $H^{(het)}$ . Similar to connectors used in multimodal learning (Liu et al., 2023), we use a **Covariate Homogenizer (CH)**, a simple linear layer, to transform  $H^{(het)}$  into latent homogeneous covariates  $C^{(het)}$ . These covariates encapsulate the temporal dynamics of high-level features derived from heterogeneous covariates:

$$C_{1:T+H}^{(het)} = \text{CH}(H_{1:T+H}^{(het)}), \quad (2)$$

where  $C_{1:T+H}^{(het)} \in \mathbb{R}^{(T+H) \times d^{het}}$ , with  $d^{het}$  being a tunable hyperparameter. Finally, all homogeneous covariates—whether hidden or observed—are aligned along the temporal dimension and concatenated to produce a cohesive set of homogeneous series covariates  $C_{1:T+H} \leftarrow [C_{1:T+H}, C_{1:T+H}^{(het)}]$ , enabling their integration into a unified covariate fusion framework. In the following part, we assume the unified covariates representation  $C_{1:T+H} \in \mathbb{R}^{(T+H) \times M}$ , where  $M$  is the total number of homogeneous covariates, including the observed homogeneous and the homogenized heterogeneous covariates. This homogenization process ensures the **universality of UniCA**.

#### 4.2 COVARIATE FUSION MODULE

**Decomposition of TSFM.** To better incorporate covariate information into the TSFM and fully leverage its capabilities, we first decompose the TSFM architecture according to the functionality:

- **Tokenizer**:  $Z = \mathcal{T}(Y_{1:T})$ : This module transforms raw time series inputs  $Y$  into a sequence of tokens  $Z \in \mathbb{R}^{P \times d}$ , where  $d$  is the token dimension, and  $P$  is the number of tokens along the temporal dimension and varies between patch-based (Das et al., 2024; Liu et al., 2024c) and point-based (Ansari et al., 2024; Hoo et al., 2025; Shi et al., 2024) methods. The tokenizer is responsible for generating suitable representations for the temporal encoder, acting as the connection between the raw representation and the main part of the model.
- **Temporal Encoder  $H = \mathcal{E}(Z)$** : Subsequently, the encoder processes the tokenized sequence  $Z$  to extract high-level temporal patterns and dependencies. The most popular encoder is Transformer. This stage leverages the pre-trained temporal encoding capabilities of the TSFM.
- **Predictor  $\hat{Y}_{T+1:T+H} = \mathcal{P}(H)$** : Finally, the predictor utilizes the encoded representations  $H$  to generate forecasts  $\hat{Y}$  for the future horizon  $T + 1$  to  $T + H$ . For decoder-only architectures (Brown et al., 2020; Das et al., 2024), we regard the linear output layer as the predictor.

This modular decomposition is applicable to the vast majority of TSFMs, ensuring the **compatibility of UniCA** and enabling a clean separation of responsibilities and facilitating the integration of covariate information without disrupting the core temporal processing. Based on this, we propose attention-based pre/post fusion modules to incorporate past and future covariates into the TSFMs.

**Pre-Fusion Module.** Prior to the encoding stage, the pre-fusion module integrates past covariate information with the historical target values. This module enriches the tokens with historical external factors, allowing the encoder to capture the joint dynamics between the time series and its past covariates. Inspired and simplified from Lim et al. (2019), we use a *Conditional Attention Pooling (CAP)* mechanism to fuse the past information while maintaining interpretability. Concretely, given past target  $Y_{1:T}$ , past covariates  $C_{1:T}$  and the static feature  $S$ ,  $C_{1:T}$  and  $S$  are first converted to embeddings by the tokenizer of the TSFM and a newly initialized embedding layer  $\rho$ :

$$E_{C_{1:T}} = \mathcal{T}(C_{1:T}), \quad E_S = \rho(S), \quad (3)$$

270 where  $\mathbf{E}_{C_{1:T}} \in \mathbb{R}^{P \times M \times d}$ ,  $\mathbf{E}_S \in \mathbb{R}^{N \times d}$  ( $\mathbf{E}_S = \mathbf{0}$  if no static covariates provided) is the representation  
 271 of dynamic and static covariates. Then:

$$273 \quad \mathbf{Z}_{C_{1:T}} = \text{CAP}(\mathbf{E}_{C_{1:T}} \mid \mathbf{E}_S) := \text{softmax}(\mathbf{A})\mathbf{V}, \quad (4)$$

$$274 \quad \text{where } \mathbf{A} = \text{GRN}(\text{flat}(\mathbf{E}_{C_{1:T}}), \mathbf{E}_S) \text{ and } \mathbf{V} = \text{GRN}(\mathbf{E}_{C_{1:T}}).$$

275 GRN is Gated Residual Network (a residual MLP) used in Lim et al. (2019),  $\text{flat}(\cdot)$  flattens the last  
 276 two dimension of  $\mathbf{E}_{C_{1:T}}$ ,  $\mathbf{A} \in \mathbb{R}^{P \times 1 \times M}$  is the attention affinity on each feature,  $\mathbf{V} \in \mathbb{R}^{P \times M \times d}$ .  
 277 Then, a Gated Linear Unit (GLU) Dauphin et al. (2017) is used to further trade off the influence of  
 278 covariates  $\mathbf{Z}_c$ :

$$279 \quad \tilde{\mathbf{Z}} = \mathbf{Z} + \text{GLU}(\mathbf{Z}_{C_{1:T}}). \quad (5)$$

280 This fused representation is then forwarded to the temporal encoder to produce  $\tilde{\mathbf{H}} \in \mathbb{R}^{P \times d}$ :

$$282 \quad \tilde{\mathbf{H}} = \mathcal{E}(\tilde{\mathbf{Z}}). \quad (6)$$

284 **Post-Fusion Module.** The future-known covariates  $\mathbf{C}_{T+1:T+H}$  provide direct insight into future  
 285 conditions, making them particularly valuable for forecasting. Therefore, we choose to use a post-  
 286 fusion module to incorporate future covariate information into the encoded representations  $\mathbf{H}$  after  
 287 the temporal extraction process. This step is crucial when future exogenous factors are expected to  
 288 influence the forecast. We first tokenize the future-known covariates:

$$289 \quad \mathbf{E}_{C_{T+1:T+H}} = \mathcal{T}(\mathbf{C}_{T+1:T+H}), \quad (7)$$

291 where  $\mathbf{E}_{C_{T+1:T+H}}$  represents the tokenized future covariates. We then apply the conditional attention  
 292 pooling mechanism to selectively aggregate the most relevant aspects of these future covariates at  
 293 each time step. Formally,

$$294 \quad \mathbf{Z}_{C_{T+1:T+H}} = \text{CAP}(\mathbf{E}_{C_{T+1:T+H}} \mid \mathbf{E}_S). \quad (8)$$

295 Once the most relevant future information is selected and fused, we integrate it with the past se-  
 296 quence by feeding both into a self-attention layer. This step enables the model to learn contextual  
 297 dependencies between past and future covariates, allowing for an enriched representation that better  
 298 captures the interplay between historical and forward-looking information. Mathematically, the final  
 299 fused representation is obtained as:

$$300 \quad [\hat{\mathbf{H}}, \hat{\mathbf{Z}}_{C_{T+1:T+H}}] = \text{SelfAttn}([\tilde{\mathbf{H}}, \mathbf{Z}_{C_{T+1:T+H}}]). \quad (9)$$

301 Then we predict the future target  $\hat{\mathbf{Y}}$  with the predictor  $\mathcal{P}$ :

$$302 \quad \hat{\mathbf{Y}}_{T+1:T+H} = \mathcal{P}(\hat{\mathbf{H}}). \quad (10)$$

304 Similar to adapters (Houlsby et al., 2019) in LLM, our UniCA is a plug-in module that keeps the  
 305 pretrained model parameters unchanged, thus **preserving generalization** capabilities of TSFMs.

### 306 4.3 LOSS FUNCTION

308 A key design principle of UniCA is its seamless compatibility with diverse TSFMs. We train the  
 309 UniCA adaptation modules using the same loss function the foundation model was originally pre-  
 310 trained with. This aligns the adaptation process with the TSFM’s inherent objective. Specifically, we  
 311 employ the quantile loss (Wen et al., 2017; Lim et al., 2019) for Chronos and TimesFM, the Huber  
 312 loss (Huber, 1992) for Time-MoE, and Negative Log Likelihood (NLL) for Moirai. For training sta-  
 313 bility across series of varying scales, we normalize each target instance by its historical mean and  
 314 standard deviation, following the instance normalization approach in Kim et al. (2021).

## 316 5 EXPERIMENTS

318 **Metrics.** Following the evaluation in (Aksu et al., 2024; Zhou et al., 2021), we consider four met-  
 319 rics to evaluate the performance of forecasters: Mean Absolute Percentage Error (MAPE), Mean  
 320 Square Error (MSE), Mean Absolute Error (MAE) for point forecasting ability, and Continuous  
 321 Ranked Probability Score (CRPS) for probabilistic forecasting, which is implemented as the mean  
 322 Weighted Quantile Loss (WQL) (Park et al., 2022). In all experiments, the WQL is computed on  
 323 quantile levels  $\{0.1, 0.2, \dots, 0.9\}$ . For methods generating sample forecasts, we compute the quan-  
 324 tiles based on 256 samples, whereas quantile forecasting methods are trained on the same quantile

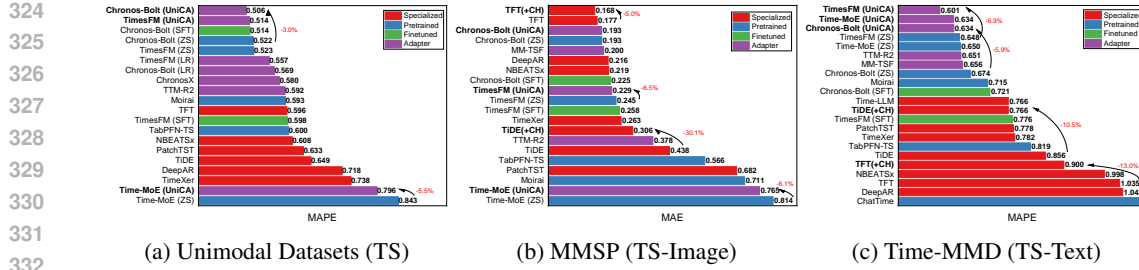


Figure 3: Forecasting performance on general covariate-aware forecasting datasets, including 12 unimodal datasets and multi-modal datasets MMSP and Time-MMD. Results are reported as MAPE averaged over sub-datasets for both unimodal and Time-MMD datasets. For the MMSP dataset, MAE is used instead, as near-zero target values render MAPE unstable.

levels we use for evaluation. Following the practice in Woo et al. (2024) to reduce the dataset bias, we normalize each result by dividing the result of the **Naive** method (Hyndman & Athanasopoulos, 2018), where all forecasts have the value of the last observation.

**Compared Methods.** To comprehensively evaluate the effectiveness of our proposed UniCA framework, we compare it against a broad set of baseline methods spanning four major categories: (a) **Specialized Models**: These models are trained from scratch for specific forecasting tasks. We include two representative subtypes: (i) *univariate methods*, which include **PatchTST** (Nie et al., 2023) and (ii) *covariate-aware methods*, which includes **DeepAR** (Salinas et al., 2020), **TFT** (Lim et al., 2019), **TIDE** (Das et al., 2023), **N-BEATsX** (Olivares et al., 2021), **TimeXer** (Wang et al., 2024b). (b) **Pretrained TSFM (ZS)**: They are evaluated in a *zero-shot* manner without task-specific fine-tuning. We select three popular TSFMs – **Chronos-Bolt** (Ansari et al., 2024), **TimesFM** (Das et al., 2024), **Time-MoE** (Shi et al., 2024). (c) **Fine-tuned TSFM (SFT)**: Full-parameter fine-tuning on downstream datasets. (d) **Adapter-based Models**: These methods introduce additional modules attached to the TSFM to inject covariate information, allowing adaptation with fewer trainable parameters. We compare the **Linear Regression (LR) adaptation** proposed in (Ansari et al., 2024; Das et al., 2024), which regresses the ground truth against covariates and the residuals are fed to TSFMs, **TTM-R2** (Ekambaram et al., 2024), **ChronosX**<sup>2</sup> (Pineda-Arango et al., 2025). For **multi-modal** experiments, we include **FusionSF** (Ma et al., 2024) and **MM-TSF** (Chronos-Bolt as TS predictor) (Liu et al., 2024a) for TS-image task (MMSP); **Time-LLM** (Jin et al., 2024), **MM-TSF** and **ChatTime** (Wang et al., 2025) for TS-text task (Time-MMD).

**Implementation Details.** We adopt default context length for each TSFM, *e.g.* 2048 for Chronos-Bolt and 4096 for Time-MoE, while prediction lengths are dataset-specific (Appendix A). All time series data is pre-processed such as normalization, as detailed in Appendix C.3. In all experiments, learning rates were selected from  $\{10^{-3}, 10^{-4}, 10^{-5}, 10^{-6}\}$  based on validation performance. The homogenizer CH is implemented as a simple linear model. For each heterogeneous covariate, we select the number of projected hidden series  $d^{het}$  in  $\{1, 2, 4, 8, 16\}$ . For image covariates, we use a simple 4-layer CNN (Krizhevsky et al., 2012) because the satellite images with dimension  $64 \times 64 \times 4$  are not regular images. For text covariates, we use GIST (Solatorio, 2024) as the encoder. A comprehensive list of hyperparameters is presented in Appendix C.7.

### 5.1 UNI-MODAL COVARIATE AWARE FORECASTING

**Datasets.** We evaluate our method on 12 publicly available datasets commonly employed in covariate-aware forecasting research (Lim et al., 2019; Das et al., 2023; Oreshkin et al., 2019; Pineda-Arango et al., 2025; Aksu et al., 2024; Olivares et al., 2021). To create the test sets, we employ two distinct strategies based on the number of subseries in each dataset. For datasets with a relatively large number of subseries, *i.e.*, we reserve the final “prediction length” points of each subseries as the test set (Lim et al., 2019). For datasets with fewer subseries, we partition 10% of the data as the test set and apply a sliding window approach for evaluation, with a step size of 1 (Zhou et al., 2021). We also spare validation sets with the same points as the test set. Detailed descriptions of the datasets can be found in Appendix A.

<sup>2</sup>This method is especially designed for Chronos-T5 model. Results obtained from our own implementation, as official code for ChronosX was not available at the time of this work.

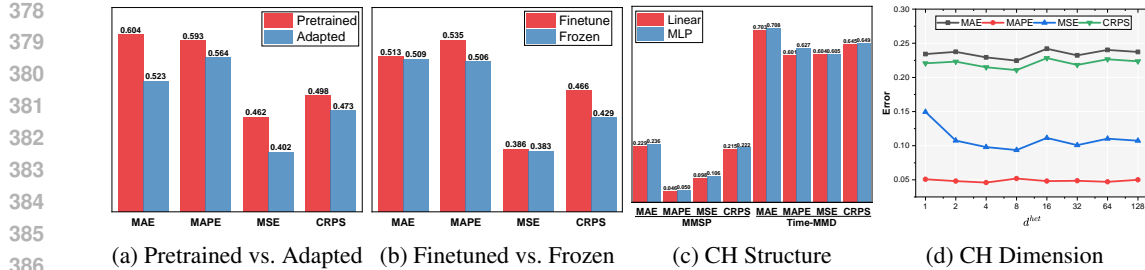


Figure 4: Average relative MAPE on unimodal datasets with model setups (a) **Pretrained**: Moirai(ZS), **Adapted**: Moirai (UniCA). (b) **Finetuned**: Chronos-Bolt (UniCA) with fine-tuned backbone, **Frozen**:freeze backbone; Ablation on (c) structure of covariate homogenizer. (d) hidden dimension of covariate homogenizer.

**Main results.** The results in Figure 3a highlight the effectiveness of UniCA in uni-modal covariate-aware forecasting. UniCA consistently outperforms zero-shot TSFMs, achieving optimal performance among adapter methods (0.506 MAPE for Chronos-Bolt). While standard finetuning shows minimal gains or degradation, UniCA delivers substantial improvements, confirming its ability to *preserve generalization*. UniCA also surpasses specialized methods (0.596-0.738 MAPE), demonstrating *universality* across architectures. These results validate UniCA’s design goals of *compatibility*, *universality*, and *generalization preservation*.

## 5.2 MULTI-MODAL COVARIATE-AWARE FORECASTING

**Datasets.** We evaluated UniCA on tasks involving multi-modal covariates, specifically images and text. For image-based covariates, we utilized the Multimodal Solar Power (MMSP) dataset from (Ma et al., 2024). For text-based covariates, we used the Time-MMD (Liu et al., 2024a) dataset. Details are in the Appendix A. Traditional covariate models use no multi-modal information.

**Main results.** On the Time-MMD dataset (figure 3c), TimesFM (UniCA) ranks among the top performers, significantly outperforming most specialized and pretrained baselines. In the MMSP benchmark (figure 3b), TFT variants achieve the best results, while our UniCA-enhanced models show consistent improvements over their base versions. *Notably, UniCA provides substantial gains for TimesFM (6.5% reduction in error) and Chronos-Bolt (5.9% reduction), confirming its effectiveness in multi-modal covariates modeling.* This suggests that multi-modal covariates can hinder forecasting performance if not handled appropriately, but our UniCA framework can robustly control the information flow through its attention-based fusion module and covariate homogenization, leading to consistent performance improvements across different foundation models.

**Homogenizer on Specialized Methods.** To evaluate the generalizability of the Covariate Homogenizer (CH), we integrate it into two representative covariate-based forecasting models to support multi-modal forecasting: TFT and TiDE. The models augmented with CH consistently outperform their vanilla counterparts. For instance, TFT+CH achieves a notable 5% drop on MMSP and 13.0% on Time-MMD. Similarly, TiDE+CH demonstrates a substantial improvement, with the MAE reduced by 30.1% on MMSP and 10.5% on Time-MMD. *These results highlight that CH provides a simple yet effective way to integrate multimodal information.*

## 5.3 ANALYSIS

**Efficiency.** The homogenizer of the UniCA uses a linear layer. The pre-/post- fusion module computes the covariate weights and pooling with the weights, introducing complexity only linear to the number of covariates and the model’s dimension. All the components are lightweight. Figure 5a shows that UniCA introduces little computation or storage burden for the TSFMs.

**Effectiveness of Covariate Adaptation.** Figure 4 highlights the effectiveness of the adapter-based covariate integration strategy in leveraging the generalization capabilities of pre-trained TSFM models. In figure 4a, we observe that the Adapted variant—using our proposed UniCA adapter—consistently outperforms the Pretrained zero-shot model (Moirai(ZS)) across all metrics. This indicates that *the diverse reliance of covariates on different datasets is difficult to learn with a pretrained model*. Adaptation with UniCA provides better performance. However, the pre-

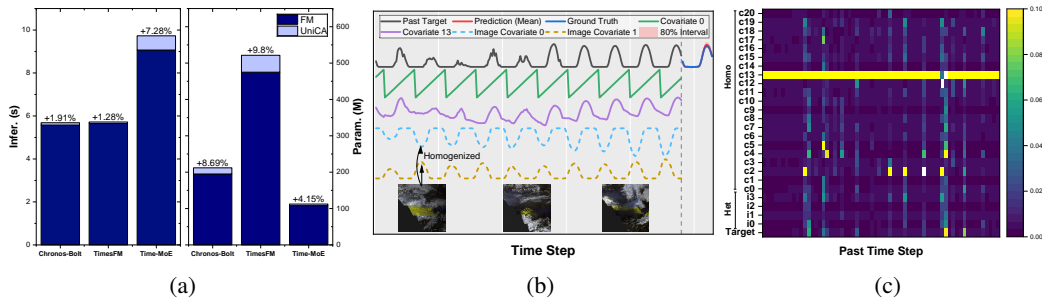


Figure 5: Analysis of UniCA. (a) **Efficiency on Time-MMD**: The adapter adds minimal overhead in inference time (left panel) and trainable parameters (right panel). (b) **Covariate Homogenization on MMSP**: Aligned heterogeneous covariates reveal meaningful patterns like seasonality and trends. (c) **Attention Maps**: The fusion module dynamically attends to different covariates over time for the sample in (b).

trained knowledge should not be fully discarded. In figure 4b, compared to fully finetuned backbones, the Frozen + Adapter setup achieves better performance, particularly in terms of MAPE and CRPS. These findings validate our design intuition: adapter-based covariate incorporation serves as a lightweight yet powerful mechanism to bridge the gap between general-purpose time series representations and task-specific covariate contexts, fully utilizing pretrained knowledge while enabling covariate-aware forecasting.

**Homogenizer Architecture.** Our evaluation of the homogenizer architecture, detailed in figure 4c, shows that a simple Linear layer and a Multi-Layer Perceptron (MLP) achieve similar performance. Notably, the Linear model slightly outperforms the MLP, indicating that a more parsimonious design is not only sufficient but preferable. Therefore, we use the Linear homogenizer as the default.

**Homogenizer Dimension.** We conduct an ablation study on the homogenized dimension  $d^{\text{het}}$ , which controls the projection space for diverse covariates. Varying  $d^{\text{het}}$  from 1 to 128, we evaluate performance using MAE, MAPE, MSE, and CRPS. As shown in Figure 4d, performance improves sharply from  $d^{\text{het}} = 1$  to 4 (e.g., MSE drops from 0.15 to under 0.10), highlighting the benefit of a more expressive projection. Increasing  $d^{\text{het}}$  beyond 8 yields diminishing returns and slight performance degradation, suggesting redundancy or overfitting. Metrics remain stable in the range [4, 32]. We set  $d^{\text{het}} = 4$  by default.

**Visualization of Covariate Homogenization.** To illustrate UniCA’s behavior and the effect of covariate homogenization, we visualize examples from the MMSP dataset (figure 5b). The homogenized representations of satellite images reveal meaningful temporal patterns: *Image Covariate 1* captures periodicity, while *Image Covariate 0* also reflects trends aligned with target scale. This shows that homogenization effectively transforms heterogeneous covariates into task-relevant representations, validating our alignment design in UniCA.

**Attention-based Covariate Selection.** Figure 5c shows attention maps before and after fusion for the same sample in figure 5b. The fusion module dynamically adjusts attention weights across time; notably, Covariate 13 consistently receives the highest weights, matching its rich temporal patterns and strong correlation with the target. In contrast, the target itself is not overly emphasized, suggesting the fusion module learns to complement, rather than duplicate, target signals—demonstrating its ability to identify and integrate informative covariates.

## 6 CONCLUSION

In this work, we address a critical limitation of existing Time Series Foundation Models (TSFMs): their inability to incorporate homogeneous and heterogeneous covariates in general forecasting effectively. To overcome this, we propose **UniCA**, a unified covariate adaptation framework that extends TSFMs to general covariate-aware forecasting scenarios. UniCA achieves this by transforming diverse covariates into high-order homogeneous series and integrates them via an attention-based fusion module, preserving the integrity of pretrained temporal modeling. Extensive experiments on both unimodal and multimodal datasets demonstrate UniCA’s compatibility, universality, and effectiveness across diverse forecasting tasks. A discussion of its limitations and future directions is provided in Appendix I.

486 7 ETHICS STATEMENT  
487488 This work complies with the ICLR Code of Ethics . Our study focuses on methodological contributions  
489 to time series forecasting with heterogeneous covariates. All experiments are conducted on  
490 publicly available benchmark datasets (e.g., M5, Retail, MMSP, Time-MMD), which do not contain  
491 personally identifiable or sensitive information. No human subjects or private data were involved,  
492 and thus no additional ethical approval was required. We have taken care to ensure that our meth-  
493 ods and findings do not pose foreseeable risks of harm, discrimination, or misuse. We believe this  
494 research aligns with the principles of responsible stewardship, fairness, transparency, and repro-  
495 ducibility.496 497 8 REPRODUCIBILITY STATEMENT  
498499 We have made extensive efforts to ensure reproducibility of our results. Detailed descriptions of the  
500 model architecture, training procedures, hyperparameters, and evaluation protocols are provided in  
501 the main paper and Appendix. We also include ablation studies and additional results in the supple-  
502 mentary materials to validate robustness. All datasets used in our experiments are publicly acces-  
503 sible, with preprocessing steps clearly documented. To further support reproducibility, we provide  
504 anonymous source code and scripts, enabling verification and extension of our findings.505 506 REFERENCES  
507508 Taha Aksu, Gerald Woo, Juncheng Liu, Xu Liu, Chenghao Liu, Silvio Savarese, Caiming Xiong,  
509 and Doyen Sahoo. Gift-eval: A benchmark for general time series forecasting model evaluation.  
510 *CoRR*, abs/2410.10393, 2024.511 Alexander Alexandrov, Konstantinos Benidis, Michael Bohlke-Schneider, Valentin Flunkert, Jan  
512 Gasthaus, Tim Januschowski, Danielle C. Maddix, Syama Rangapuram, David Salinas, Jasper  
513 Schulz, Lorenzo Stella, Ali Caner Türkmen, and Yuyang Wang. GluonTS: Probabilistic and  
514 Neural Time Series Modeling in Python. *Journal of Machine Learning Research*, 21(116):1–6,  
515 2020. URL <http://jmlr.org/papers/v21/19-820.html>.516 Abdul Fatir Ansari, Lorenzo Stella, Ali Caner Türkmen, Xiyuan Zhang, Pedro Mercado, Huibin  
517 Shen, Oleksandr Shchur, Syama Sundar Rangapuram, Sebastian Pineda-Arango, Shubham  
518 Kapoor, Jasper Zschiegner, Danielle C. Maddix, Michael W. Mahoney, Kari Torkkola, An-  
519 drew Gordon Wilson, Michael Bohlke-Schneider, and Yuyang Wang. Chronos: Learning the  
520 language of time series. *CoRR*, abs/2403.07815, 2024.521 522 Shaojie Bai, J. Zico Kolter, and Vladlen Koltun. An empirical evaluation of generic convolutional  
523 and recurrent networks for sequence modeling. *CoRR*, abs/1803.01271, 2018.524 525 G. E. P. Box and G. M. Jenkins. Some recent advances in forecasting and control. *Journal of the*  
526 *Royal Statistical Society. Series C (Applied Statistics)*, 17(2):91–109, 1968.527 528 George EP Box, Gwilym M Jenkins, Gregory C Reinsel, and Greta M Ljung. *Time series analysis:*  
529 *forecasting and control*. John Wiley & Sons, 2015.530 531 Tom B. Brown, Benjamin Mann, Nick Ryder, Melanie Subbiah, Jared Kaplan, Prafulla Dhari-  
532 wal, Arvind Neelakantan, Pranav Shyam, Girish Sastry, Amanda Askell, Sandhini Agarwal,  
533 Ariel Herbert-Voss, Gretchen Krueger, Tom Henighan, Rewon Child, Aditya Ramesh, Daniel M.  
534 Ziegler, Jeffrey Wu, Clemens Winter, Christopher Hesse, Mark Chen, Eric Sigler, Mateusz Litwin,  
535 Scott Gray, Benjamin Chess, Jack Clark, Christopher Berner, Sam McCandlish, Alec Radford,  
Ilya Sutskever, and Dario Amodei. Language models are few-shot learners. In *NeurIPS*, 2020.536 537 Jiawei Chen and Chunhui Zhao. Addressing spatial-temporal heterogeneity: Gen-  
538 539 eral mixed time series analysis via latent continuity recovery and alignment. In  
*Advances in Neural Information Processing Systems*, volume 37, 2024. URL  
[https://proceedings.neurips.cc/paper\\_files/paper/2024/file/1feb87871436031bdc0f2beaa62a049b-Paper-Conference.pdf](https://proceedings.neurips.cc/paper_files/paper/2024/file/1feb87871436031bdc0f2beaa62a049b-Paper-Conference.pdf).

540 Kyunghyun Cho, Bart van Merriënboer, Dzmitry Bahdanau, and Yoshua Bengio. On the properties  
 541 of neural machine translation: Encoder-decoder approaches. In *SSST@EMNLP*, pp. 103–111.  
 542 Association for Computational Linguistics, 2014.

543

544 Corporación Favorita. Corporación favorita grocery sales forecasting competition, 2018. URL  
 545 <https://www.kaggle.com/c/favorita-grocery-sales-forecasting/>.

546 Abhimanyu Das, Weihao Kong, Andrew Leach, Shaan Mathur, Rajat Sen, and Rose Yu. Long-term  
 547 forecasting with tide: Time-series dense encoder. *CoRR*, abs/2304.08424, 2023.

548

549 Abhimanyu Das, Weihao Kong, Rajat Sen, and Yichen Zhou. A decoder-only foundation model for  
 550 time-series forecasting. In *ICML*. OpenReview.net, 2024.

551 Yann N. Dauphin, Angela Fan, Michael Auli, and David Grangier. Language modeling with gated  
 552 convolutional networks. In *ICML*, volume 70 of *Proceedings of Machine Learning Research*, pp.  
 553 933–941. PMLR, 2017.

554

555 Jacob Devlin, Ming-Wei Chang, Kenton Lee, and Kristina Toutanova. BERT: pre-training of deep  
 556 bidirectional transformers for language understanding. In *NAACL-HLT*, pp. 4171–4186, 2019.

557 Kumar Dheenadayalan, Nitesh Kumar, Suprabath Reddy, and Sumant Kulkarni. Multimodal neu-  
 558 ral network for demand forecasting. In *ICONIP*, volume 13625 of *Lecture Notes in Computer  
 559 Science*, pp. 409–421. Springer, 2022.

560

561 Vijay Ekambaram, Arindam Jati, Nam Nguyen, Phanwadee Sinthong, and Jayant Kalagnanam.  
 562 Tsmixer: Lightweight mlp-mixer model for multivariate time series forecasting. In *KDD*, pp.  
 563 459–469, 2023.

564 Vijay Ekambaram, Arindam Jati, Pankaj Dayama, Sumanta Mukherjee, Nam Nguyen, Wesley M.  
 565 Gifford, Chandra Reddy, and Jayant Kalagnanam. Tiny time mixers (ttms): Fast pre-trained mod-  
 566 els for enhanced zero/few-shot forecasting of multivariate time series. In *2024*, 2024.

567

568 Mostafa Farrokhabadi, Jethro Browell, Yi Wang, Stephen Makonin, Wencong Su, and Hamidreza  
 569 Zareipour. Day-ahead electricity demand forecasting competition: Post-covid paradigm. *IEEE  
 570 Open Access Journal of Power and Energy*, 9:185–191, 2022. doi: 10.1109/OAJPE.2022.  
 571 3161101.

572 Jean-Yves Franceschi, Aymeric Dieuleveut, and Martin Jaggi. Unsupervised scalable representation  
 573 learning for multivariate time series. In *NeurIPS*, pp. 4652–4663, 2019.

574

575 Mononito Goswami, Konrad Szafer, Arjun Choudhry, Yifu Cai, Shuo Li, and Artur Dubrawski. MO-  
 576 MENT: A family of open time-series foundation models. In *Forty-first International Conference  
 577 on Machine Learning, ICML 2024, Vienna, Austria, July 21-27, 2024*. OpenReview.net, 2024.

578 Aleksandra Gruca, Federico Serva, Llorenç Lliso, Pilar Rípodas, Xavier Calbet, Pedro Herruzo,  
 579 Jiří Piht, Rudolf Raeovskyi, Petr Šimánek, Matej Choma, et al. Weather4cast at neurips 2022:  
 580 Super-resolution rain movie prediction under spatio-temporal shifts. In *NeurIPS 2022 Competi-  
 581 tion Track*, pp. 292–313. PMLR, 2022.

582 Nate Gruver, Marc Finzi, Shikai Qiu, and Andrew Gordon Wilson. Large language models are  
 583 zero-shot time series forecasters. In *NeurIPS*, 2023.

584

585 Lu Han, Han-Jia Ye, and De-Chuan Zhan. The capacity and robustness trade-off: Revisiting the  
 586 channel independent strategy for multivariate time series forecasting. *IEEE Transactions on  
 587 Knowledge and Data Engineering*, 36(11):7129–7142, 2024.

588 Sepp Hochreiter and Jürgen Schmidhuber. Long short-term memory. *Neural computation*, 9(8):  
 589 1735–1780, 1997.

590

591 Noah Hollmann, Samuel Müller, Lennart Purucker, Arjun Krishnakumar, Max Körfer, Shi Bin Hoo,  
 592 Robin Tibor Schirrmeyer, and Frank Hutter. Accurate predictions on small data with a tabular  
 593 foundation model. *Nature*, 01 2025. doi: 10.1038/s41586-024-08328-6. URL <https://www.nature.com/articles/s41586-024-08328-6>.

594 Tao Hong, Pierre Pinson, and Shu Fan. Global energy forecasting competition 2012. *International*  
 595 *Journal of Forecasting*, 30:357–363, 2014. URL <https://api.semanticscholar.org/CorpusID:54890724>.

596

597 Tao Hong, Pierre Pinson, Shu Fan, Hamidreza Zareipour, Alberto Troccoli, and Rob J Hyndman. Probabilistic energy forecasting: Global energy forecasting competition 2014 and beyond. *International Journal of Forecasting*, 32:896–913, 2016. URL <https://api.semanticscholar.org/CorpusID:155534780>.

600

601

602 Tao Hong, Jingrui Xie, and Jonathan D. Black. Global energy forecasting competition 2017: Hierarchical probabilistic load forecasting. *International Journal of Forecasting*, 2019. URL <https://api.semanticscholar.org/CorpusID:159389280>.

603

604

605 Shi Bin Hoo, Samuel Müller, David Salinas, and Frank Hutter. The tabular foundation model  
 606 tabpfn outperforms specialized time series forecasting models based on simple features. *CoRR*,  
 607 abs/2501.02945, 2025.

608

609 Neil Houlsby, Andrei Giurgiu, Stanislaw Jastrzebski, Bruna Morrone, Quentin de Laroussilhe, An-  
 610 drea Gesmundo, Mona Attariyan, and Sylvain Gelly. Parameter-efficient transfer learning for  
 611 NLP. In *ICML*, volume 97 of *Proceedings of Machine Learning Research*, pp. 2790–2799. PMLR,  
 612 2019.

613

614 Edward J. Hu, Yelong Shen, Phillip Wallis, Zeyuan Allen-Zhu, Yuanzhi Li, Shean Wang, Lu Wang,  
 615 and Weizhu Chen. Lora: Low-rank adaptation of large language models. In *ICLR*. OpenRe-  
 view.net, 2022.

616

617 Peter J Huber. Robust estimation of a location parameter. In *Breakthroughs in statistics: Methodol-*  
 618 *ogy and distribution*, pp. 492–518. Springer, 1992.

619

620 Rob J Hyndman and George Athanasopoulos. *Forecasting: principles and practice*. OTexts, 2018.

621

622 Nicholas J. Hourly energy demand, generation, and weather  
 623 data. <https://www.kaggle.com/datasets/nicholasjhana/energy-consumption-generation-prices-and-weather>, 2019. Accessed:  
 624 2025-05-09.

625

626 Ming Jin, Shiyu Wang, Lintao Ma, Zhixuan Chu, James Y. Zhang, Xiaoming Shi, Pin-Yu Chen,  
 627 Yuxuan Liang, Yuan-Fang Li, Shirui Pan, and Qingsong Wen. Time-lm: Time series forecasting  
 628 by reprogramming large language models. In *ICLR*. OpenReview.net, 2024.

629

630 Akhil Kadiyala and Ashok Kumar. Multivariate time series models for prediction of air quality  
 631 inside a public transportation bus using available software. *Environmental Progress & Sustainable*  
 632 *Energy*, 33(2):337–341, 2014.

633

634 Evaggelos G Kardakos, Minas C Alexiadis, Stylianos I Vagropoulos, Christos K Simoglou, Pan-  
 635 delis N Biskas, and Anastasios G Bakirtzis. Application of time series and artificial neural network  
 636 models in short-term forecasting of pv power generation. In *2013 48th International Universities'*  
 637 *Power Engineering Conference (UPEC)*, pp. 1–6. IEEE, 2013.

638

639 Taesung Kim, Jinhee Kim, Yunwon Tae, Cheonbok Park, Jang-Ho Choi, and Jaegul Choo. Re-  
 640 versible instance normalization for accurate time-series forecasting against distribution shift. In  
 641 *ICLR*, 2021.

642

643 Alexander Kirillov, Eric Mintun, Nikhila Ravi, Hanzi Mao, Chloé Rolland, Laura Gustafson, Tete  
 644 Xiao, Spencer Whitehead, Alexander C. Berg, Wan-Yen Lo, Piotr Dollár, and Ross B. Girshick.  
 645 Segment anything. In *IEEE/CVF International Conference on Computer Vision, ICCV 2023, Paris, France, October 1-6, 2023*, pp. 3992–4003. IEEE, 2023.

646

647 Alex Krizhevsky, Ilya Sutskever, and Geoffrey E. Hinton. Imagenet classification with deep convolutional neural networks. In *NIPS*, pp. 1106–1114, 2012.

648

649 Jesus Lago, Grzegorz Marcjasz, Bart De Schutter, and Rafal Weron. Forecasting day-ahead electric-  
 650 ity prices: A review of state-of-the-art algorithms, best practices and an open-access benchmark.  
 651 *Applied Energy*, 293:116983, 2021.

648 Bryan Lim, Sercan Ömer Arik, Nicolas Loeff, and Tomas Pfister. Temporal fusion transformers for  
 649 interpretable multi-horizon time series forecasting. *CoRR*, abs/1912.09363, 2019.  
 650

651 Haotian Liu, Chunyuan Li, Qingyang Wu, and Yong Jae Lee. Visual instruction tuning. In *NeurIPS*,  
 652 2023.

653 Haixin Liu, Shangqing Xu, Zhiyuan Zhao, Lingkai Kong, Harshavardhan Kamarthi, Aditya B. Sasa-  
 654 nur, Megha Sharma, Jiaming Cui, Qingsong Wen, Chao Zhang, and B. Aditya Prakash. Time-  
 655 mmd: Multi-domain multimodal dataset for time series analysis. In *NeurIPS*, 2024a.  
 656

657 Yong Liu, Tengge Hu, Haoran Zhang, Haixu Wu, Shiyu Wang, Lintao Ma, and Mingsheng Long.  
 658 itransformer: Inverted transformers are effective for time series forecasting. In *ICLR*. OpenRe-  
 659 view.net, 2024b.

660 Yong Liu, Guo Qin, Xiangdong Huang, Jianmin Wang, and Mingsheng Long. Timer-xl: Long-  
 661 context transformers for unified time series forecasting. *CoRR*, abs/2410.04803, 2024c.  
 662

663 Ziqing Ma, Wenwei Wang, Tian Zhou, Chao Chen, Bingqing Peng, Liang Sun, and Rong Jin. Fu-  
 664 sionsf: Fuse heterogeneous modalities in a vector quantized framework for robust solar power  
 665 forecasting. In *SIGKDD*, pp. 5532–5543. ACM, 2024.

666 Spyros Makridakis, Evangelos Spiliotis, and Vassilios Assimakopoulos. The m5 competition: Back-  
 667 ground, organization, and implementation. *International Journal of Forecasting*, 38(4):1325–  
 668 1336, 2022.

669 Clayton Miller, Anjukan Kathirgamanathan, Bianca Picchetti, Pandarasamy Arjunan, June Young  
 670 Park, Zoltán Nagy, Paul Raftery, Brodie W. Hobson, Zixiao Shi, Forrest Meggers National Univer-  
 671 sity of Singapore, University College Dublin, Comision Nacional de Energia Atomica. Argentina.,  
 672 Berkeley Education Alliance for Research in Singapore, The University of Texas at Austin, Uni-  
 673 versity of California Berkeley, C. Zhang Cardiff University, and Princeton University. The build-  
 674 ing data genome project 2, energy meter data from the ashrae great energy predictor iii competi-  
 675 tion. *Scientific Data*, 7, 2020. URL <https://api.semanticscholar.org/CorpusID:219259693>.

676 Mohammad Amin Morid, Olivia R Liu Sheng, and Joseph Dunbar. Time series prediction using  
 677 deep learning methods in healthcare. *ACM Transactions on Management Information Systems*,  
 678 14(1):1–29, 2023.

679 Yuqi Nie, Nam H. Nguyen, Phanwadee Sinthong, and Jayant Kalagnanam. A time series is worth  
 680 64 words: Long-term forecasting with transformers. In *ICLR*, 2023.

681 David Obst, Badih Ghattas, Sandra Clauzel, Jairo Cugliari, Yannig Goude, and Georges Oppenheim.  
 682 Textual data for time series forecasting. *CoRR*, abs/1910.12618, 2019.

683 Kin G. Olivares, Cristian Challu, Grzegorz Marcjasz, Rafal Weron, and Artur Dubrawski. Neural  
 684 basis expansion analysis with exogenous variables: Forecasting electricity prices with nbeatsx.  
 685 *CoRR*, abs/2104.05522, 2021.

686 Boris N Oreshkin, Dmitri Carpow, Nicolas Chapados, and Yoshua Bengio. N-BEATS: Neural basis  
 687 expansion analysis for interpretable time series forecasting. In *ICLR*, 2019.

688 Youngsuk Park, Danielle C. Maddix, François-Xavier Aubet, Kelvin Kan, Jan Gasthaus, and Yuyang  
 689 Wang. Learning quantile functions without quantile crossing for distribution-free time series  
 690 forecasting. In *AISTATS*, volume 151 of *Proceedings of Machine Learning Research*, pp. 8127–  
 691 8150. PMLR, 2022.

692 Yu Peng, Miao Lei, Jia Guo, and Xiyuan Peng. Multiresolution analysis and forecasting of mobile  
 693 communication traffic. *Chinese Journal of Electronics*, 22(2):373–376, 2013.

694 Sebastian Pineda-Arango, Pedro Mercado, Shubham Kapoor, Abdul Fatir Ansari, Lorenzo Stella,  
 695 Huibin Shen, Hugo Senetaire, Caner Turkmen, Oleksandr Shchur, Danielle C. Maddix, Michael  
 696 Bohlke-Schneider, Yuyang Wang, and Syama Sundar Rangapuram. Chronosx: Adapting pre-  
 697 trained time series models with exogenous variables. *CoRR*, abs/2503.12107, 2025.

702 Alec Radford, Jeff Wu, Rewon Child, David Luan, Dario Amodei, and Ilya Sutskever. Language  
 703 models are unsupervised multitask learners. 2019.

704

705 Alec Radford, Jong Wook Kim, Chris Hallacy, Aditya Ramesh, Gabriel Goh, Sandhini Agarwal,  
 706 Girish Sastry, Amanda Askell, Pamela Mishkin, Jack Clark, Gretchen Krueger, and Ilya Sutskever.  
 707 Learning transferable visual models from natural language supervision. In *ICML*, volume 139 of  
 708 *Proceedings of Machine Learning Research*, pp. 8748–8763. PMLR, 2021.

709 Syama Sundar Rangapuram, Matthias W. Seeger, Jan Gasthaus, Lorenzo Stella, Yuyang Wang, and  
 710 Tim Januschowski. Deep state space models for time series forecasting. In *NeurIPS*, pp. 7796–  
 711 7805, 2018.

712 David Salinas, Valentin Flunkert, Jan Gasthaus, and Tim Januschowski. DeepAR: Probabilistic  
 713 forecasting with autoregressive recurrent networks. *International Journal of Forecasting*, 36(3):  
 714 1181–1191, 2020.

715

716 Xiaoming Shi, Shiyu Wang, Yuqi Nie, Dianqi Li, Zhou Ye, Qingsong Wen, and Ming Jin. Time-  
 717 moe: Billion-scale time series foundation models with mixture of experts. *CoRR*, abs/2409.16040,  
 718 2024.

719 Aivin V. Solatorio. Gistembed: Guided in-sample selection of training negatives for text embedding  
 720 fine-tuning. *CoRR*, abs/2402.16829, 2024.

721

722 Hugo Touvron, Louis Martin, Kevin Stone, Peter Albert, Amjad Almahairi, Yasmine Babaei, Niko-  
 723 lay Bashlykov, Soumya Batra, Prajjwal Bhargava, Shruti Bhosale, Dan Bikel, Lukas Blecher,  
 724 Cristian Canton-Ferrer, Moya Chen, Guillem Cucurull, David Esiobu, Jude Fernandes, Jeremy  
 725 Fu, Wenjin Fu, Brian Fuller, Cynthia Gao, Vedanuj Goswami, Naman Goyal, Anthony Hartshorn,  
 726 Saghar Hosseini, Rui Hou, Hakan Inan, Marcin Kardas, Viktor Kerkez, Madian Khabsa, Isabel  
 727 Kloumann, Artem Korenev, Punit Singh Koura, Marie-Anne Lachaux, Thibaut Lavril, Jenya Lee,  
 728 Diana Liskovich, Yinghai Lu, Yuning Mao, Xavier Martinet, Todor Mihaylov, Pushkar Mishra,  
 729 Igor Molybog, Yixin Nie, Andrew Poulton, Jeremy Reizenstein, Rashi Rungta, Kalyan Saladi,  
 730 Alan Schelten, Ruan Silva, Eric Michael Smith, Ranjan Subramanian, Xiaoqing Ellen Tan, Bin  
 731 Tang, Ross Taylor, Adina Williams, Jian Xiang Kuan, Puxin Xu, Zheng Yan, Iliyan Zarov, Yuchen  
 732 Zhang, Angela Fan, Melanie Kambadur, Sharan Narang, Aurélien Rodriguez, Robert Stojnic,  
 733 Sergey Edunov, and Thomas Scialom. Llama 2: Open foundation and fine-tuned chat models.  
*CoRR*, abs/2307.09288, 2023.

734 Chengsen Wang, Qi Qi, Jingyu Wang, Haifeng Sun, Zirui Zhuang, Jinming Wu, Lei Zhang, and  
 735 Jianxin Liao. Chattime: A unified multimodal time series foundation model bridging numerical  
 736 and textual data. In *AAAI*, pp. 12694–12702. AAAI Press, 2025.

737

738 Xinlei Wang, Maike Feng, Jing Qiu, Jinjin Gu, and Junhua Zhao. From news to forecast: Integrating  
 739 event analysis in llm-based time series forecasting with reflection. In *NeurIPS*, 2024a.

740

741 Yuxuan Wang, Haixu Wu, Jiaxiang Dong, Guo Qin, Haoran Zhang, Yong Liu, Yunzhong Qiu, Jian-  
 742 min Wang, and Mingsheng Long. Timexer: Empowering transformers for time series forecasting  
 743 with exogenous variables. In *NeurIPS*, 2024b.

744

745 Zhixian Wang, Qingsong Wen, Chaoli Zhang, Liang Sun, Leandro Von Krannichfeldt, and Yi Wang.  
 746 Benchmarks and custom package for electrical load forecasting. *CoRR*, abs/2307.07191, 2023.

747

748 Ruofeng Wen, Kari Torkkola, Balakrishnan Narayanaswamy, and Dhruv Madeka. A multi-horizon  
 749 quantile recurrent forecaster. *CoRR*, abs/1711.11053, 2017.

750

751 Gerald Woo, Chenghao Liu, Akshat Kumar, Caiming Xiong, Silvio Savarese, and Doyen Sahoo.  
 752 Unified training of universal time series forecasting transformers. In *ICML*. OpenReview.net,  
 753 2024.

754

755 Ashfak Yeafi. Pdb electric power load history. <https://www.kaggle.com/datasets/ashfakyeafi/pbd-load-history>, 2021. Accessed: 2025-05-09.

756

757 Haoyi Zhou, Shanghang Zhang, Jieqi Peng, Shuai Zhang, Jianxin Li, Hui Xiong, and Wancai Zhang.  
 758 Informer: Beyond efficient transformer for long sequence time-series forecasting. In *AAAI*, pp.  
 759 11106–11115, 2021.

756 Tian Zhou, Peisong Niu, Xue Wang, Liang Sun, and Rong Jin. One fits all: Power general time  
 757 series analysis by pretrained LM. In *NeurIPS*, 2023.  
 758

# 763 Appendix

## 766 Table of Contents

768 Appendices	<b>15</b>
769	
770 <b>A Datasets Descriptions</b>	<b>16</b>
771 A.1 Uni-modal Time Series Datasets . . . . .	16
772 A.2 Multi-modal Datasets . . . . .	16
773	
774 <b>B Compared Methods</b>	<b>17</b>
775 B.1 Specialized Method . . . . .	17
776 B.2 Pretrained Method . . . . .	18
777 B.3 Multimodal Metehod . . . . .	19
778 B.4 Finetuned Method . . . . .	19
779 B.5 Adapter Method . . . . .	19
780	
781 <b>C Implementation Details</b>	<b>20</b>
782 C.1 Code availability . . . . .	20
783 C.2 Compute Resource Information . . . . .	20
784 C.3 Preprocessing . . . . .	21
785 C.4 Architecture of TSFM . . . . .	21
786 C.5 Algorithm of UniCA . . . . .	21
787 C.6 Optimization . . . . .	22
788 C.7 Hyperparamters . . . . .	23
789	
790 <b>D Experiment Details</b>	<b>23</b>
791 D.1 Train-Test Splitting. . . . .	23
792 D.2 Evaluation Metrics . . . . .	23
793	
794	
795 <b>E Full Results</b>	<b>25</b>
796 E.1 Robustness Evaluation via Error Bars. . . . .	25
797 E.2 Unimodal Forecasting . . . . .	25
798 E.3 Multi-Modal Forecasting . . . . .	28
799 E.4 Imputation . . . . .	29
800	
801 <b>F Showcases</b>	<b>29</b>
802	
803 <b>G More Ablation</b>	<b>31</b>
804 G.1 Fusion Position. . . . .	31
805 G.2 Influence of Modality Encoder . . . . .	31
806 G.3 Architecture of Covariate Homogenizer . . . . .	36
807 G.4 Influence of Static Covariates . . . . .	36
808 G.5 Impact of Covariates . . . . .	38
809 G.6 Robustness to Noisy Covariates . . . . .	39

810	G.7 Fusion Architecture . . . . .	39
811		
812	<b>H Correlation Analysis of Homogenized Covariate Embeddings</b>	<b>40</b>
813		
814	<b>I Discussion of Limitation</b>	<b>41</b>
815		
816	<b>J The Use of LLMs</b>	<b>41</b>

## 819 A DATASETS DESCRIPTIONS

### 821 A.1 UNI-MODAL TIME SERIES DATASETS

823 Our study employed 12 uni-modal datasets with covariates. Detailed descriptions of the targets,  
 824 covariates, and data sources are provided in Table 1, while Table 2 outlines the dataset statistics.  
 825 Specifically, a selection of electricity load forecasting datasets, including Covid19 Energy,  
 826 GEF12, GEF17, PDB, Spain, BDG-2 Hog, BDG-2 Bull, and BDG-2 Cockatoo, was directly re-  
 827 trieval from the Lotsa repository on Hugging Face: [https://huggingface.co/datasets/Salesforce/lotsa\\_data](https://huggingface.co/datasets/Salesforce/lotsa_data). An exception to this is the GEF14 dataset, which we acquired from  
 828 its original source (Hong et al., 2016) due to the absence of covariate data in the version available  
 829 on Hugging Face.

831 **Table 1: Dataset Descriptions**

Dataset Name	Descriptions	Covariates	Source
EPF	Day-ahead electricity prices from five major power markets: Nord pool, PJM, FR, BE, and DE	load forecasts, wind generation	(Lago et al., 2021)
M5-daily	M5 competition using 30K hierarchical sales data from Walmar three states CA, TX and WI to forecast the daily sales for the next 28 days.	store ID, item ID, sell prices, week day, month, year, SNAP CA, SNAP TX, SNAP WI, event type	(Makridakis et al., 2022)
Retail	Corporación Favorita Grocery Sales Forecasting competition hosted in Kaggle.	store no., item no., on promotion, oil prices, week day, month, year, holidays events,	(Corporación Favorita, 2018)
BDG-2 Hog	The Building Data Genome 2 (BDG2) dataset in the Hog region. An open dataset that includes non-residential building-level data collected from 3053 electricity meters, which covers 1636 buildings.	air temperature, drew temperature, sea level pressure, wind direction, wind speed	(Miller et al., 2020; Wang et al., 2023; Woo et al., 2024)
BDG-2 Bull	BDG-2 dataset collected from Univ. of Texas at Austin.	air temperature, wind speed sea level pressure	(Miller et al., 2020; Wang et al., 2023; Woo et al., 2024)
BDG-2 Cockatoo	BDG-2 dataset collected from Cornell University.	air temperature	(Miller et al., 2020; Wang et al., 2023; Woo et al., 2024)
Covid19 Energy	3+ years of load data from the Day-Ahead Electricity Demand Forecasting Competition. The purpose is to study the impact of the Covid-19 on the power system.	air temperature	(Farrokhbadi et al., 2022; Wang et al., 2023)
GFC12	20 aggregated-level load series data from the Global Energy Forecasting Competition 2012	Randomly selected second temperature data because there is no one-to-one correspondance between the temperature and load data	(Hong et al., 2014; Wang et al., 2023; Woo et al., 2024)
GFC14	Seven years of load series data from the Global Energy Forecasting Competition 2014	Averaged temperature from the raw 25 temperature data series.	(Hong et al., 2016)
GFC17	Eight load data from year 2016 to 2017 originally from the Global Energy Forecasting Competition 2014	air temperature	(Hong et al., 2019; Wang et al., 2023; Woo et al., 2024)
PDB	Two years of PDB electric power load history data from the Kaggle data competition.	air temperature	(Yeafi, 2021; Wang et al., 2023; Woo et al., 2024)
Spain	Hourly energy demand generation and weather in five major cities in Spain. It is a Kaggle data competition.	air temperature of Barcelona	(J., 2019; Wang et al., 2023; Woo et al., 2024)

### 850 A.2 MULTI-MODAL DATASETS

853 To evaluate our approach, we utilized two distinct multi-modal datasets: Time-MMD (Liu et al.,  
 854 2024a) and the Multimodal Solar Power (MMSP) dataset (Ma et al., 2024).

855 The Time-MMD dataset is a multi-domain resource encompassing nine diverse areas such as Agriculture, Climate, Health, and Traffic. It features paired textual and time series data, where the textual  
 856 information is derived from curated reports and web search results, as detailed in (Liu et al., 2024a).  
 857 Among the original 9 subsets, we exclude 2 sets (Agriculture and Economy) because we find no  
 858 specialized method can outperform the Naive method, thus they may be unpredictable. We reserved  
 859 20% of each dataset as the test set. Time-MMD allows for the investigation of models capable of  
 860 integrating information across different modalities and domains.

862 The MMSP dataset comprises one and a half years of solar power generation records collected from  
 863 88 individual plants. We select the first 10 series as in (Ma et al., 2024). Crucially, it includes temporally  
 864 aligned heterogeneous covariates for each plant, consisting of satellite imagery and numerical

864  
865 Table 2: Dataset Statistics. Dynamic covariates and past dynamic covariates are covariates that are  
866 observed and unobserved in the forecasting horizon, respectively.  
867

| 867<br>868<br>869<br>870<br>871<br>872<br>873<br>874<br>875<br>876<br>877 |
|---|---|---|---|---|---|---|---|---|---|
| Dataset Name  | Domain  | Num. Series   | Freq.   | Categorical Cov.  |   | Real Cov.   |   | Num. Obs.   | Pred. Len.  |
|   |   |   |   | Static  | Dynamic   | Dynamic   | Past Dynamic  |   |   |
| EPF   | Energy/Price  | 5   | H   | 0   | 0   | 0   | 2   | 218,280   | 48  |
| M5-daily  | Sales   | 30,490  | D   | 5   | 8   | 1   | 0   | 59,181,090  | 28  |
| Retail  | Sales   | 119,048   | D   | 7   | 4   | 0   | 2   | 140,246,203   | 8   |
| BDG-2 Bull  | Energy/Load   | 41  | H   | 0   | 0   | 0   | 3   | 719,304   | 48  |
| BDG-2 Cockatoo  | Energy/Load   | 1   | H   | 0   | 0   | 0   | 1   | 17,544  | 48  |
| Covid19 Energy  | Energy/Load   | 1   | H   | 0   | 0   | 0   | 1   | 31,912  | 48  |
| GFC12   | Energy/Load   | 20  | H   | 0   | 0   | 0   | 1   | 788,280   | 48  |
| GFC14   | Energy/Load   | 1   | H   | 0   | 0   | 0   | 1   | 60,600  | 48  |
| GFC17   | Energy/Load   | 8   | H   | 0   | 0   | 0   | 1   | 140,352   | 48  |
| BDG-2 Hog   | Energy/Load   | 24  | H   | 0   | 0   | 0   | 5   | 421,056   | 48  |
| PDB   | Energy/Load   | 1   | H   | 0   | 0   | 0   | 1   | 17,520  | 48  |
| Spain   | Energy/Load   | 1   | H   | 0   | 0   | 0   | 1   | 35,064  | 48  |

878  
879 Table 3: Multi-modal Dataset Descriptions  
880

881 882 883 884 885 886 887 888 889 890 891 892 893 894 895 896 897 898 899 900	881 882 883 884 885 886 887 888 889 890 891 892 893 894 895 896 897 898 899 900	881 882 883 884 885 886 887 888 889 890 891 892 893 894 895 896 897 898 899 900	881 882 883 884 885 886 887 888 889 890 891 892 893 894 895 896 897 898 899 900	Multi-Modal Covariates			881 882 883 884 885 886 887 888 889 890 891 892 893 894 895 896 897 898 899 900	881 882 883 884 885 886 887 888 889 890 891 892 893 894 895 896 897 898 899 900	
				Text	Image	Time Series			
Time-MMD	Time-MMD	Time-MMD	Time-MMD	Agriculture: retail broiler composite	USDA Broiler Market News Report; Daily National Broiler Market at a Glance, etc.	N/A	N/A	17,520	12
				Climate: US Precipitation Index	Drought Report National Climate Report	N/A	N/A	496	12
				Economy: US trade in goods with World	U.S. International Trade in Goods and Services Economic Indicators Report	N/A	N/A	423	12
				Energy: gasoline price	Annual Energy Outlook from EIA; Weekly Petroleum Status Report	N/A	N/A	1479	12
				Social Good: unemployment statistics in the US	monthly employment situations; annual labor force characteristics by race and ethnicity	N/A	N/A	900	12
				Public Health: InfluenzaLike Illness statistics	Weekly U.S. Influenza Surveillance Report Annual Flu Season Key Studies and News Reports	N/A	N/A	1389	12
				Environment: Outdoor air quality	Daily News	N/A	N/A	11,102	12
				Traffic: Traffic Volume Trends	Weekly Traffic Volume Report	N/A	N/A	531	12
				Security: Disaster and Emergency Grants	Billion-Dollar Weather and Climate Disasters; Disaster and emergency declarations	N/A	N/A	297	12
				Energy: Solar Power Generation	N/A	Satellite Images	Numerical Weather Predictions, (Latitude, Longitude)	1,129,920	24

901  
902 weather predictions. This dataset provides a challenging real-world scenario for multi-modal learning-  
903 ing, requiring the fusion of visual and numerical information to predict power output.  
904

## 905 B COMPARED METHODS

906 In this section, we provide an overview of the baseline methods employed in our experiments, with  
907 a focus on their methodological frameworks and covariate handling strategies. Each approach is an-  
908 alyzed in terms of its integration of homogeneous covariates, highlighting strengths and limitations  
909 in modeling external dependencies.  
910

### 911 B.1 SPECIALIZED METHOD

912 **PatchTST (Nie et al., 2023)** PatchTST is a model that transforms time series into patches, which  
913 are then encoded using a Transformer to produce forecasts. It involves two main components: Patch-  
914 ing and Channel Independence. Patching divides time series into subseries-level patches, serving as  
915 input tokens to the Transformer. This preserves local temporal patterns while minimizing compu-  
916

tational complexity for attention maps, enabling longer history modeling. Channel Independence ensures that each channel uses the same embedding and Transformer weights, treating multivariate inputs as separate but parallel sequences. PatchTST does not incorporate covariate information in forecasting.

**NBEATS (Oreshkin et al., 2019)** NBEATS (Neural Basis Expansion Analysis for Time Series Forecasting) is a deep learning model designed for univariate time series forecasting. Its core idea is to decompose the time series into interpretable components, typically trend and seasonality, using stack-based architecture where each stack consists of multiple blocks. Each block learns to forecast a portion of the input series using basis expansion functions (approximated by fully connected layers) and subtracts its forecast from the input, passing the residual to the next block or stack. This iterative residual learning allows NBEATS to model complex patterns and achieve strong forecasting performance, often outperforming statistical and hybrid methods, while also offering some interpretability through its decomposition into basis function.

**NBEATSx (Olivares et al., 2021)** An extension of the purely univariate NBEATS model, NBEATSx incorporates covariates by appending them to the backcast and forecast layers in each neural block. It uses a dual-stack architecture (generic + interpretable) to model both nonlinear dependencies and explicit covariate effects. This makes it effective for scenarios where future covariates (e.g., planned events) are known.

**DeepAR (Salinas et al., 2020)** Developed by Amazon, DeepAR is a probabilistic RNN-based model that explicitly integrates covariates. Each time step’s dynamic covariates (e.g., temperature, price) are concatenated with the target variable and fed into the RNN. It assumes covariates are known for both training and prediction, making it ideal for applications like demand forecasting where external factors (e.g., marketing campaigns) drive outcomes.

**TFT (Lim et al., 2019)** Developed by Google, the Temporal Fusion Transformer (TFT) uses a modular design to integrate static covariates (e.g., store IDs), known future inputs (e.g., holidays), and observed variables (e.g., sales). It processes past covariates in the encoder and future covariates in the decoder via gated recurrent networks and variable selection networks. This hierarchical approach ensures robustness to missing or noisy covariates while maintaining interpretability.

**TiDE (Das et al., 2023)** TiDE (Time-series Dense Encoder) is a deep learning model for multi-variate time series forecasting, distinguished by its efficient, MLP-only architecture. It processes the historical lookback window of the target series and any available past covariates through a dense encoder to learn a latent representation. A separate MLP-based decoder then uses this representation, along with linearly projected future covariate information, to generate multi-step forecasts.

**TimeXer (Wang et al., 2024b)** TimeXer is a Transformer-based time series model that processes time series as sequences of patches. It uses a hierarchical structure with patch embedding, temporal encoding, and attention mechanisms to capture both short-term and long-term dependencies. TimeXer handles the covariates by employing the “variate-level embedding”. External covariates are embedded and then integrated directly into the patch representations of the target time series. This allows the model to learn how these external factors influence the internal time series dynamics at the patch level, enabling the model to account for the impact of these exogenous variables in its predictions.

## B.2 PRETRAINED METHOD

**Moirai (Woo et al., 2024)**<sup>3</sup> Moirai, a time series foundation model from Salesforce, is engineered for universal forecasting across diverse time series data. At its core, Moirai utilizes a Transformer-based architecture and is pre-trained on a massive and varied dataset called LOTSA. A key architectural component is its ability to handle any number and type of covariates, both those known in the future and those that are not. Moirai achieves this by conditioning its probabilistic forecast generation, which uses a flexible output distribution, on these covariates, allowing the model to produce forecasts that are informed by the provided exogenous variables.

<sup>3</sup><https://huggingface.co/Salesforce/moirai-1.1-R-small>

972 **TabPFN-TS (Hoo et al., 2025)** <sup>4</sup> TabPFN-TS, a regression variant of the TabPFN(Hollmann et al.,  
 973 2025) model to time series, is a foundation model pre-trained on pure artificial datasets, enabling  
 974 few-shot time series forecasting. When incorporating covariate data, TabPFN-TS typically treats  
 975 these exogenous variables as additional features. These covariate features are then concatenated  
 976 with the temporal information before being processed by its Transformer-based architecture, which  
 977 is adapted for tabular data. The model’s pre-training on tabular data allows it to potentially learn  
 978 complex relationships between all input features, including the covariates, even with limited time  
 979 series-specific training.

980 **Time-MoE** See section C.4 for the model details.

981 **Chronos-Bolt** See section C.4 for the model details.

982 **TimesFM** See section C.4 for the model details.

### 983 B.3 MULTIMODAL METEHOD

984 **Time-LLM** Time-LLM (Jin et al., 2024) is a foundation model that adapts a pre-trained Large  
 985 Language Model (LLM) for general-purpose time series analysis. Instead of full fine-tuning, it  
 986 employs a lightweight “reprogramming” layer. This layer transforms input time series into a text-  
 987 prototype format that the frozen LLM can process. By aligning the LLM’s inherent sequence model-  
 988 ing capabilities with statistical time series patterns, Time-LLM can perform diverse tasks like fore-  
 989 casting, classification, and anomaly detection through simple text prompts, leveraging the LLM’s  
 990 reasoning abilities while remaining computationally efficient.

991 **ChatTime** ChatTime (Wang et al., 2025) is a multimodal time series foundation model designed  
 992 as a single, end-to-end language model that directly processes interleaved sequences of numerical  
 993 time series data and natural language. It introduces key innovations, including a unified time series  
 994 tokenizer that represents time series patches as discrete tokens and a temporal-aware attention mech-  
 995 anism to effectively capture complex temporal dependencies. By training on this mixed-modality  
 996 input, ChatTime can perform diverse analysis tasks like forecasting and classification through a  
 997 conversational interface, directly interpreting and responding to queries about the provided data. We  
 998 used the checkpoint ChengsenWang/ChatTime-1-7B-Chat<sup>5</sup> released by the authors in our exper-  
 999 iment.

### 1000 B.4 FINETUNED METHOD

1001 Supervised Fine-Tuning (SFT) is the process of adapting a pre-trained Time Series Foundation  
 1002 Model (TSFM) to a specific downstream task or dataset by further training it on target-specific  
 1003 labeled data. This allows the model to leverage its general time series understanding learned during  
 1004 pre-training and specialize its parameters for improved performance on the new, specific time se-  
 1005 ries. In our implementation, we utilized the target time series without the covariates and adopted the  
 1006 same hyperparameters (e.g., learning rate) and data split as UniCA for consistency. During training,  
 1007 the model adjusts its pre-learned weights to better align with the characteristics of the target series,  
 1008 enhancing specialization for the task at hand.

### 1009 B.5 ADAPTER METHOD

1010 **Linear Regression (LR) Adapter.** In our experiments, we leveraged exogenous variables using a  
 1011 linear regression methodology inspired by the approaches of the Chronos(Ansari et al., 2024) and  
 1012 TimeFM(Das et al., 2024) time series foundation models. This regressor approach involves decom-  
 1013 posing the target series into two components: contributions from the covariates and the target itself.  
 1014 Initially, we perform a regression of the target variable against the known covariates. Subsequently,  
 1015 we subtract the predicted target values from the actual target values to compute the residuals. These  
 1016 residuals serve as the context for the time series foundation models, which forecast future residuals.

1024 <sup>4</sup><https://huggingface.co/Prior-Labs/TabPFN-v2-reg>

1025 <sup>5</sup><https://huggingface.co/ChengsenWang/ChatTime-1-7B-Chat>

1026 Table 4: Overview of the baseline models, grouped by type and implementation source. We utilized  
 1027 implementations from the popular time series libraries GluonTS and NeuralForecast, or the official  
 1028 author repository (marked as “Reference”). All experiments were conducted using the default hy-  
 1029 perparameters provided by the respective implementation.

1031	Model	Type	Implementation
1032	PatchTST	Specialized	GluonTS
1033	NBEATS	Specialized	GluonTS
1034	DeepAR	Specialized	GluonTS
1035	TFT	Specialized	GluonTS
1036	TiDE	Specialized	GluonTS
1037	NBEATSx	Specialized	NeuralForecast
1038	TimeXer	Specialized	NeuralForecast
1039	Moirai	Pretrained	Reference
1040	TimesFM	Pretrained	Reference
1041	TabPFN-TS	Pretrained	Reference
1042	TTM-R2	Pretrained/Adapter	Reference
1043	FusionSF	Multimodal	Reference
1044	Time-LLM	Multimodal	Reference
1045	ChatTime	Multimodal	Reference

1046  
 1047  
 1048 The ultimate forecasts are obtained by summing the predicted residuals with the target forecasts  
 1049 derived from the covariates.

1050 A notable limitation of the covariate regressor approach is its reliance on covariates that are known  
 1051 over the forecasting horizon, such as dynamic categorical and dynamic real covariates. Past covari-  
 1052 ates, including past dynamic categorical and past dynamic real covariates, are only available for the  
 1053 context window. To address this limitation, we employ the corresponding TSFM to forecast these  
 1054 past covariates into the horizon, thus extending their utility beyond the context window.

1055  
 1056 **TTM (Ekambaram et al., 2024)** <sup>6</sup> Tiny Time Mixers (TTM) are compact models for multivari-  
 1057 ate time series forecasting, featuring only 1 million parameters. Built on the efficient TSMixer ar-  
 1058 chitecture, TTM use MLPMixer blocks with simple gated attention, offering a faster alternative  
 1059 to traditional Transformer self-attention mechanisms. TTM are pre-trained on diverse, large-scale  
 1060 datasets from Monash and LibCity, encompassing various domains and temporal scales. TTM’s ar-  
 1061 chitecture addresses data heterogeneity through innovations such as Adaptive Patching for adjusting  
 1062 patch lengths, Diverse Resolution Sampling for enhancing generalization across resolutions, and  
 1063 Resolution Prefix Tuning for embedding resolution info in training. This approach allows TTM to  
 1064 excel in resource-limited settings by initially training models channel-independently, followed by  
 1065 fine-tuning to integrate target and exogenous channel correlations.

## 1066 C IMPLEMENTATION DETAILS

### 1069 C.1 CODE AVAILABILITY

1071 Our code has been made anonymous and is available at [https://anonymous.4open.  
 1072 science/r/UniCA-C5E0](https://anonymous.4open.science/r/UniCA-C5E0).

### 1074 C.2 COMPUTE RESOURCE INFORMATION

1076 For all the experiments, we use 4 GeForce RTX 3090. For baselines, we used cpu instances with 40  
 1077 virtual cpus and 384 GiB of memory. The library requirement for reproducing the results is available  
 1078 on the above repository.

1079 <sup>6</sup><https://huggingface.co/ibm-granite/granite-timeseries-ttm-r2>

1080  
1081

## C.3 PREPROCESSING

1082  
1083  
1084  
1085  
1086  
1087  
1088  
1089  
1090

We mainly follow the series preprocessing pipeline proposed in TFT (Lim et al., 2019). We impute missing values in both the target and covariate series using forward filling and add a corresponding binary indicator to mark the imputed timesteps. The time features are generated based on the time series frequency (e.g., hour, weekday, month as periodic features). Then, the time features are vertically stacked with known dynamic features to form a unified feature matrix. Missing static features are filled with a default value of zero. Finally, each time series is assigned a unique identifier to distinguish it in multi-series forecasting. This ensures that the resulting data format meets the input requirements of deep learning models, providing a normalized representation for time series forecasting.

1091  
1092  
1093  
1094  
1095  
1096

## C.4 ARCHITECTURE OF TSFM

1097  
1098  
1099  
1100  
1101  
1102  
1103  
1104

In this section, we detail the tokenization, encoding, and decoding procedures of two time series foundation models: Chronos and TimesFM. These decomposition steps provide a clearer understanding of their internal mechanisms and differences.

1105  
1106  
1107  
1108  
1109  
1110  
1111  
1112  
1113

**Chronos-Bolt (Ansari et al., 2024).** <sup>7</sup> Chronos-Bolt adopts an encoder-decoder architecture based on T5. During tokenization, the input time series undergoes instance normalization. It is then segmented into patches along with its mask, and the two streams are concatenated before embedding. An optional [REG] token can be added to support regression-style outputs. The encoder transforms the tokenized inputs via a stack of T5 encoders, generating contextualized hidden states. These are fed to the decoder, which performs sequence generation conditioned on attention masks, and yields multiple quantile forecasts. Extended prediction lengths are handled through decoding extrapolation. All outputs are rescaled back using stored normalization parameters.

1114  
1115  
1116  
1117  
1118  
1119  
1120  
1121  
1122  
1123

**TimesFM (Das et al., 2024).** <sup>8</sup> TimesFM utilizes a Transformer decoder-only architecture. The tokenization stage includes preprocessing, fixed-length patching, and normalization via mean and standard deviation. Patches are augmented with mask features and projected into embedding space, optionally with positional encodings. The encoder applies multi-layer self-attention to obtain contextual representations. The decoder operates in an auto-regressive manner, iteratively generating future values. Outputs include both mean and quantile predictions, which are de-normalized to restore the original scale. TimesFM also supports frequency-based conditioning and hybrid-frequency modeling for improved multi-scale forecasting.

1124  
1125  
1126  
1127  
1128  
1129  
1130  
1131  
1132  
1133

**Time-MoE (Shi et al., 2024)** <sup>9</sup> Time-MoE is the first billion-scale time-series foundation model that marries a decoder-only Transformer with a sparse mixture-of-experts (MoE) backbone to boost capacity without proportional inference cost. Each Transformer block replaces the dense feed-forward layer with a shared pool of eight experts, and a learned router sparsely activates just two experts per token, while rotary positional embeddings and RMSNorm enhance stability. The authors pre-train three variants—Time-MoE-base (50 M activated / 113 M total parameters), Time-MoE-large (200 M / 453 M) and Time-MoE-ultra (1.1 B activated / 2.4 B total)—all support channel-independent forecasting for arbitrary horizons via a multi-resolution head. Training uses Huber loss and the newly curated Time-300B corpus:  $\approx$  48 M sequences and  $>$  300 billion time points drawn from nine domains.

## C.5 ALGORITHM OF UNICA

1134  
1135  
1136  
1137  
1138  
1139  
1140  
1141  
1142  
1143  
1144  
1145  
1146  
1147  
1148  
1149  
1150  
1151  
1152  
1153  
1154  
1155  
1156  
1157  
1158  
1159  
1160  
1161  
1162  
1163  
1164  
1165  
1166  
1167  
1168  
1169  
1170  
1171  
1172  
1173  
1174  
1175  
1176  
1177  
1178  
1179  
1180  
1181  
1182  
1183  
1184  
1185  
1186  
1187  
1188  
1189  
1190  
1191  
1192  
1193  
1194  
1195  
1196  
1197  
1198  
1199  
1200  
1201  
1202  
1203  
1204  
1205  
1206  
1207  
1208  
1209  
1210  
1211  
1212  
1213  
1214  
1215  
1216  
1217  
1218  
1219  
1220  
1221  
1222  
1223  
1224  
1225  
1226  
1227  
1228  
1229  
1230  
1231  
1232  
1233  
1234  
1235  
1236  
1237  
1238  
1239  
1240  
1241  
1242  
1243  
1244  
1245  
1246  
1247  
1248  
1249  
1250  
1251  
1252  
1253  
1254  
1255  
1256  
1257  
1258  
1259  
1260  
1261  
1262  
1263  
1264  
1265  
1266  
1267  
1268  
1269  
1270  
1271  
1272  
1273  
1274  
1275  
1276  
1277  
1278  
1279  
1280  
1281  
1282  
1283  
1284  
1285  
1286  
1287  
1288  
1289  
1290  
1291  
1292  
1293  
1294  
1295  
1296  
1297  
1298  
1299  
1300  
1301  
1302  
1303  
1304  
1305  
1306  
1307  
1308  
1309  
1310  
1311  
1312  
1313  
1314  
1315  
1316  
1317  
1318  
1319  
1320  
1321  
1322  
1323  
1324  
1325  
1326  
1327  
1328  
1329  
1330  
1331  
1332  
1333  
1334  
1335  
1336  
1337  
1338  
1339  
1340  
1341  
1342  
1343  
1344  
1345  
1346  
1347  
1348  
1349  
1350  
1351  
1352  
1353  
1354  
1355  
1356  
1357  
1358  
1359  
1360  
1361  
1362  
1363  
1364  
1365  
1366  
1367  
1368  
1369  
1370  
1371  
1372  
1373  
1374  
1375  
1376  
1377  
1378  
1379  
1380  
1381  
1382  
1383  
1384  
1385  
1386  
1387  
1388  
1389  
1390  
1391  
1392  
1393  
1394  
1395  
1396  
1397  
1398  
1399  
1400  
1401  
1402  
1403  
1404  
1405  
1406  
1407  
1408  
1409  
1410  
1411  
1412  
1413  
1414  
1415  
1416  
1417  
1418  
1419  
1420  
1421  
1422  
1423  
1424  
1425  
1426  
1427  
1428  
1429  
1430  
1431  
1432  
1433  
1434  
1435  
1436  
1437  
1438  
1439  
1440  
1441  
1442  
1443  
1444  
1445  
1446  
1447  
1448  
1449  
1450  
1451  
1452  
1453  
1454  
1455  
1456  
1457  
1458  
1459  
1460  
1461  
1462  
1463  
1464  
1465  
1466  
1467  
1468  
1469  
1470  
1471  
1472  
1473  
1474  
1475  
1476  
1477  
1478  
1479  
1480  
1481  
1482  
1483  
1484  
1485  
1486  
1487  
1488  
1489  
1490  
1491  
1492  
1493  
1494  
1495  
1496  
1497  
1498  
1499  
1500  
1501  
1502  
1503  
1504  
1505  
1506  
1507  
1508  
1509  
1510  
1511  
1512  
1513  
1514  
1515  
1516  
1517  
1518  
1519  
1520  
1521  
1522  
1523  
1524  
1525  
1526  
1527  
1528  
1529  
1530  
1531  
1532  
1533  
1534  
1535  
1536  
1537  
1538  
1539  
1540  
1541  
1542  
1543  
1544  
1545  
1546  
1547  
1548  
1549  
1550  
1551  
1552  
1553  
1554  
1555  
1556  
1557  
1558  
1559  
1560  
1561  
1562  
1563  
1564  
1565  
1566  
1567  
1568  
1569  
1570  
1571  
1572  
1573  
1574  
1575  
1576  
1577  
1578  
1579  
1580  
1581  
1582  
1583  
1584  
1585  
1586  
1587  
1588  
1589  
1590  
1591  
1592  
1593  
1594  
1595  
1596  
1597  
1598  
1599  
1600  
1601  
1602  
1603  
1604  
1605  
1606  
1607  
1608  
1609  
1610  
1611  
1612  
1613  
1614  
1615  
1616  
1617  
1618  
1619  
1620  
1621  
1622  
1623  
1624  
1625  
1626  
1627  
1628  
1629  
1630  
1631  
1632  
1633  
1634  
1635  
1636  
1637  
1638  
1639  
1640  
1641  
1642  
1643  
1644  
1645  
1646  
1647  
1648  
1649  
1650  
1651  
1652  
1653  
1654  
1655  
1656  
1657  
1658  
1659  
1660  
1661  
1662  
1663  
1664  
1665  
1666  
1667  
1668  
1669  
1670  
1671  
1672  
1673  
1674  
1675  
1676  
1677  
1678  
1679  
1680  
1681  
1682  
1683  
1684  
1685  
1686  
1687  
1688  
1689  
1690  
1691  
1692  
1693  
1694  
1695  
1696  
1697  
1698  
1699  
1700  
1701  
1702  
1703  
1704  
1705  
1706  
1707  
1708  
1709  
1710  
1711  
1712  
1713  
1714  
1715  
1716  
1717  
1718  
1719  
1720  
1721  
1722  
1723  
1724  
1725  
1726  
1727  
1728  
1729  
1730  
1731  
1732  
1733  
1734  
1735  
1736  
1737  
1738  
1739  
1740  
1741  
1742  
1743  
1744  
1745  
1746  
1747  
1748  
1749  
1750  
1751  
1752  
1753  
1754  
1755  
1756  
1757  
1758  
1759  
1760  
1761  
1762  
1763  
1764  
1765  
1766  
1767  
1768  
1769  
1770  
1771  
1772  
1773  
1774  
1775  
1776  
1777  
1778  
1779  
1780  
1781  
1782  
1783  
1784  
1785  
1786  
1787  
1788  
1789  
1790  
1791  
1792  
1793  
1794  
1795  
1796  
1797  
1798  
1799  
1800  
1801  
1802  
1803  
1804  
1805  
1806  
1807  
1808  
1809  
1810  
1811  
1812  
1813  
1814  
1815  
1816  
1817  
1818  
1819  
1820  
1821  
1822  
1823  
1824  
1825  
1826  
1827  
1828  
1829  
1830  
1831  
1832  
1833  
1834  
1835  
1836  
1837  
1838  
1839  
1840  
1841  
1842  
1843  
1844  
1845  
1846  
1847  
1848  
1849  
1850  
1851  
1852  
1853  
1854  
1855  
1856  
1857  
1858  
1859  
1860  
1861  
1862  
1863  
1864  
1865  
1866  
1867  
1868  
1869  
1870  
1871  
1872  
1873  
1874  
1875  
1876  
1877  
1878  
1879  
1880  
1881  
1882  
1883  
1884  
1885  
1886  
1887  
1888  
1889  
1890  
1891  
1892  
1893  
1894  
1895  
1896  
1897  
1898  
1899  
1900  
1901  
1902  
1903  
1904  
1905  
1906  
1907  
1908  
1909  
1910  
1911  
1912  
1913  
1914  
1915  
1916  
1917  
1918  
1919  
1920  
1921  
1922  
1923  
1924  
1925  
1926  
1927  
1928  
1929  
1930  
1931  
1932  
1933  
1934  
1935  
1936  
1937  
1938  
1939  
1940  
1941  
1942  
1943  
1944  
1945  
1946  
1947  
1948  
1949  
1950  
1951  
1952  
1953  
1954  
1955  
1956  
1957  
1958  
1959  
1960  
1961  
1962  
1963  
1964  
1965  
1966  
1967  
1968  
1969  
1970  
1971  
1972  
1973  
1974  
1975  
1976  
1977  
1978  
1979  
1980  
1981  
1982  
1983  
1984  
1985  
1986  
1987  
1988  
1989  
1990  
1991  
1992  
1993  
1994  
1995  
1996  
1997  
1998  
1999  
2000  
2001  
2002  
2003  
2004  
2005  
2006  
2007  
2008  
2009  
2010  
2011  
2012  
2013  
2014  
2015  
2016  
2017  
2018  
2019  
2020  
2021  
2022  
2023  
2024  
2025  
2026  
2027  
2028  
2029  
2030  
2031  
2032  
2033  
2034  
2035  
2036  
2037  
2038  
2039  
2040  
2041  
2042  
2043  
2044  
2045  
2046  
2047  
2048  
2049  
2050  
2051  
2052  
2053  
2054  
2055  
2056  
2057  
2058  
2059  
2060  
2061  
2062  
2063  
2064  
2065  
2066  
2067  
2068  
2069  
2070  
2071  
2072  
2073  
2074  
2075  
2076  
2077  
2078  
2079  
2080  
2081  
2082  
2083  
2084  
2085  
2086  
2087  
2088  
2089  
2090  
2091  
2092  
2093  
2094  
2095  
2096  
2097  
2098  
2099  
2100  
2101  
2102  
2103  
2104  
2105  
2106  
2107  
2108  
2109  
2110  
2111  
2112  
2113  
2114  
2115  
2116  
2117  
2118  
2119  
2120  
2121  
2122  
2123  
2124  
2125  
2126  
2127  
2128  
2129  
2130  
2131  
2132  
2133  
2134  
2135  
2136  
2137  
2138  
2139  
2140  
2141  
2142  
2143  
2144  
2145  
2146  
2147  
2148  
2149  
2150  
2151  
2152  
2153  
2154  
2155  
2156  
2157  
2158  
2159  
2160  
2161  
2162  
2163  
2164  
2165  
2166  
2167  
2168  
2169  
2170  
2171  
2172  
2173  
2174  
2175  
2176  
2177  
2178  
2179  
2180  
2181  
2182  
2183  
2184  
2185  
2186  
2187  
2188  
2189  
2190  
2191  
2192  
2193  
2194  
2195  
2196  
2197  
2198  
2199  
2200  
2201  
2202  
2203  
2204  
2205  
2206  
2207  
2208  
2209  
2210  
2211  
2212  
2213  
2214  
2215  
2216  
2217  
2218  
2219  
2220  
2221  
2222  
2223  
2224  
2225  
2226  
2227  
2228  
2229  
22210  
22211  
22212  
22213  
22214  
22215  
22216  
22217  
22218  
22219  
22220  
22221  
22222  
22223  
22224  
22225  
22226  
22227  
22228  
22229  
222210  
222211  
222212  
222213  
222214  
222215  
222216  
222217  
222218  
222219  
222220  
222221  
222222  
222223  
222224  
222225  
222226  
222227  
222228  
222229  
2222210  
2222211  
2222212  
2222213  
2222214  
2222215  
2222216  
2222217  
2222218  
2222219  
2222220  
2222221  
2222222  
2222223  
2222224  
2222225  
2222226  
2222227  
2222228  
2222229  
22222210  
22222211  
22222212  
22222213  
22222214  
22222215  
22222216  
22222217  
22222218  
22222219  
22222220  
22222221  
22222222  
22222223  
22222224  
22222225  
22222226  
22222227  
22222228  
22222229  
222222210  
222222211  
222222212  
222222213  
222222214  
222222215  
222222216  
222222217  
222222218  
222222219  
222222220  
222222221  
222222222  
222222223  
222222224  
222222225  
222222226  
222222227  
222222228  
222222229  
2222222210  
2222222211  
2222222212  
2222222213  
2222222214  
2222222215  
2222222216  
2222222217  
2222222218  
2222222219  
2222222220  
2222222221  
2222222222  
2222222223  
2222222224  
2222222225  
2222222226  
2222222227  
2222222228  
2222222229  
22222222210  
22222222211  
22222222212  
22222222213  
22222222214  
22222222215  
22222222216  
22222222217  
22222222218  
22222222219  
22222222220  
22222222221  
22222222222  
22222222223  
22222222224  
22222222225  
22222222226  
22222222227  
22222222228  
22222222229  
222222222210  
222222222211  
222222222212  
222222222213  
222222222214  
222222222215  
222222222216  
222222222217  
222222222218  
222222222219  
222222222220  
222222222221  
222222222222  
222222222223  
222222222224  
222222222225  
222222222226  
222222222227  
222222222228  
222222222229  
2222222222210  
2222222222211  
2222222222212  
2222222222213  
2222222222214  
2222222222215  
2222222222216  
2222222222217  
2222222222218  
2222222222219  
2222222222220  
2222222222221  
2222222222222  
2222222222223  
2222222222224  
2222222222225  
2222222222226  
2222222222227  
2222222222228  
2222222222229  
22222222222210  
22222222222211  
22222222222212  
22222222222213  
22222222222214  
22222222222215  
22222222222216  
22222222222217  
22222222222218  
22222222222219  
22222222222220  
22222222222221  
22222222222222  
22222222222223  
22222222222224  
22222222222225  
22222222222226  
22222222222227  
22222222222228  
22222222222229  
222222222222210  
222222222222211  
222222222222212  
222222222222213  
222222222222214  
222222222222215  
222222222222216  
222222222222217  
222222222222218  
222222222222219  
222222222222220  
222222222222221  
222222222222222  
222222222222223  
222222222222224  
222222222222225  
222222222222226  
222222222222227  
222222222222228  
222222222222229  
2222222222222210  
2222222222222211  
2222222222222212  
2222222222222213  
2222222222222214  
2222222222222215  
2222222222222216  
2222222222222217  
2222222222222218  
2222222222222219  
2222222222222220  
2222222222222221  
2222222222222222  
2222222222222223  
2222222222222224  
2222222222222225  
2222222222222226  
2222222222222227  
2222222222222228  
2222222222222229  
22222222222222210  
22222222222222211  
22222222222222212  
22222222222222213  
22222222222222214  
22222222222222215  
22222222222222216  
22222222222222217  
22222222222222218  
22222222222222219  
22222222222222220  
22222222222222221  
2222

1134 Table 5: Comparison between Chronos-Bolt, TimesFM and Time-MoE in terms of model architec-  
 1135 ture and processing steps.

1136

1137 <b>Component</b>	1138 <b>Chronos-Bolt</b>	1139 <b>TimesFM</b>	1140 <b>Time-MoE</b>
1141 Architecture	1142 T5-based encoder-decoder	1143 Decoder-only	1144 Decoder-only
1145 Tokenizer	1146 Patch-based Residual MLP	1147 Patch-based Residual MLP	1148 Point-based Gated Linear
1149 Encoder	1150 T5 encoder stack	1151 Custom Transformer	1152 Custom Transformer
1153 Predictor	1154 T5 decoder	1155 Residual MLP	1156 Linear
1157 Prediction Output	1158 Multiple quantile predictions	1159 Mean and quantile predictions	1160 Point predictions

1161

1162

1163 the *Pre-Fusion Module*, we integrate historical covariate information into the tokenized target se-  
 1164 quence using a conditional global attention mechanism followed by a gating unit. This enriched se-  
 1165 quence is passed to the pretrained encoder of the TSFM to extract temporal patterns. After encoding,  
 1166 the *Post-Fusion Module* incorporates future-known covariates using another attention-based fusion  
 1167 mechanism, allowing the model to dynamically select complementary covariate signals. Finally, the  
 1168 predictor of the TSFM generates the future forecasts from the fused representation. This modular  
 1169 workflow enables UniCA to flexibly and effectively adapt general-purpose TSFMs to covariate-rich  
 1170 forecasting scenarios, while preserving the pretrained temporal modeling capabilities.

1171

1172

---

**Algorithm 1** UniCA: Unified Covariate Adaptation for TSFM
 

---

1173 **Require:** Target series  $Y_{1:T}$ , static covariates  $S$ , dynamic covariates  $C_{1:T+H} = \{C_{1:T}, C_{T+1:T+H}\}$ , pretrained TSFM  $(\mathcal{T}, \mathcal{E}, \mathcal{P})$   
 1174 **Ensure:** Forecast  $\hat{Y}_{T+1:T+H}$

1175 1: **Covariate Homogenization:**  
 1176 2: **for** each heterogeneous covariate **do**  
 1177 3:   Encode modality to dense feature  $H^{(het)}$   
 1178 4:   Convert to homogeneous covariate via covariate homogenizer  $C^{(het)} = \text{CH}(H^{(het)})$   
 1179 5: **end for**  
 1180 6: Concatenate all homogeneous covariates:  $C \leftarrow \{C, C^{(het)}\}$   
 1181 7: **Pre-Fusion Module:**  
 1182 8: Tokenize past target:  $Z = \mathcal{T}(Y_{1:T})$   
 1183 9: Tokenize past covariates:  $E_{C_{1:T}} = \mathcal{T}(C_{1:T})$   
 1184 10: Embed static covariates:  $E_S = \rho(S)$   
 1185 11: Compute conditional attention:  $Z_{C_{1:T}} = \text{CondAttnPool}(E_{C_{1:T}} \mid E_S)$   
 1186 12: Fuse covariates with GLU:  $\tilde{Z} = Z + \text{GLU}(Z_{C_{1:T}})$   
 1187 13: **Temporal Encoding:**  
 1188 14: Encode fused sequence:  $\tilde{H} = \mathcal{E}(\tilde{Z})$   
 1189 15: **Post-Fusion Module:**  
 1190 16: Tokenize future covariates:  $E_{C_{T+1:T+H}} = \mathcal{T}(C_{T+1:T+H})$   
 1191 17: Compute conditional attention:  $Z_{C_{T+1:T+H}} = \text{CondAttnPool}(E_{C_{T+1:T+H}} \mid E_S)$   
 1192 18: Fuse via self-attention:  $[\hat{H}, \hat{Z}_{C_{T+1:T+H}}] = \text{SelfAttn}([\tilde{H}, Z_{C_{T+1:T+H}}])$   
 1193 19: **Forecasting:**  
 1194 20: Predict target:  $\hat{Y}_{T+1:T+H} = \mathcal{P}(\hat{H})$

---

1195

1196

1197

1198

1199

1200

1201

1202

1203

1204

1205

1206

1207

1208

1209

1210

**C.6 OPTIMIZATION**

1211

1212

1213

1214

1215

1216

1217

1218

1219

1220

1221

1222

1223

1224

1225

1226

1227

1228

1229

1230

1231

1232

1233

1234

1235

1236

1237

1238

1239

1240

1241

1242

1243

1244

1245

1246

1247

1248

1249

1250

1251

1252

1253

1254

1255

1256

1257

1258

1259

1260

1261

1262

1263

1264

1265

1266

1267

1268

1269

1270

1271

1272

1273

1274

1275

1276

1277

1278

1279

1280

1281

1282

1283

1284

1285

1286

1287

1288

1289

1290

1291

1292

1293

1294

1295

1296

1297

1298

1299

1300

1301

1302

1303

1304

1305

1306

1307

1308

1309

1310

1311

1312

1313

1314

1315

1316

1317

1318

1319

1320

1321

1322

1323

1324

1325

1326

1327

1328

1329

1330

1331

1332

1333

1334

1335

1336

1337

1338

1339

1340

1341

1342

1343

1344

1345

1346

1347

1348

1349

1350

1351

1352

1353

1354

1355

1356

1357

1358

1359

1360

1361

1362

1363

1364

1365

1366

1367

1368

1369

1370

1371

1372

1373

1374

1375

1376

1377

1378

1379

1380

1381

1382

1383

1384

1385

1386

1387

1388

1389

1390

1391

1392

1393

1394

1395

1396

1397

1398

1399

1400

1401

1402

1403

1404

1405

1406

1407

1408

1409

1410

1411

1412

1413

1414

1415

1416

1417

1418

1419

1420

1421

1422

1423

1424

1425

1426

1427

1428

1429

1430

1431

1432

1433

1434

1435

1436

1437

1438

1439

1440

1441

1442

1443

1444

1445

1446

1447

1449

1450

1451

1452

1453

1454

1455

1456

1457

1458

1459

1460

1461

To prevent overfitting, early stopping is implemented based on validation loss. Training proceeds in mini-batches, with each epoch comprising 50 gradient steps. Model checkpoints are saved corresponding to the epoch that yields the best validation performance.

### C.7 HYPERPARAMTERS

For all experiments, we search the hyperparameters listed in table 6.

Table 6: Key hyperparameters, their search spaces, or fixed values used in training UniCA across all datasets.

Hyperparameter	Value / Range	Description
Learning rate	{1e-3,1e-4,1e-5,1e-6}	Initial learning rate for Adam optimizer
Weight decay	{1e-2,1e-4,1e-6}	L2 regularization weight
Scheduler patience	5	Epochs to wait before reducing LR
Scheduler factor	0.5	Multiplicative factor for LR reduction
Batch size	{8,16,32,64}	Number of samples per training batch
Max epochs	100	Maximum number of training epochs
Early stopping patience	10	Epochs to wait for improvement before stopping
Context length	TSFM-specific	Length of input window for encoder
Prediction length	Dataset-specific	Length of prediction window
Embedding dimension	TSFM-specific	Dimension of input embeddings
Homogenizatoin dimension	{1,2,4,8,16}	Dimension of homogenized series of each heterogeneous covariate

## D EXPERIMENT DETAILS

### D.1 TRAIN-TEST SPLITTING.

The train-test follows the setups in (Aksu et al., 2024). For datasets with large number of series, *i.e.* M5 (Makridakis et al., 2022) and Retail (Lim et al., 2019), we spare the last "prediction length" of each series for test and all the observed points before the test points are used for training. For other datasets, we partition 10% of the data as the test set and apply a sliding window approach for evaluation, with a step size of 1 (Zhou et al., 2021). Among the training points, we also split the validation points.

### D.2 EVALUATION METRICS

We use four metrics to evaluate performance of forecasters: Mean Absolute Error (MAE), Mean Square Error (MSE), Mean Absolute Percentage Error (MAPE) for point forecasting ability, and Continuous Ranked Probability Score (CRPS) for probabilistic forecasting. For all metrics, we use GluonTS library implementation to calculate final values (Alexandrov et al., 2020).

**MAE** The *Mean Absolute Error* (MAE) is a commonly used evaluation metric in time series forecasting that measures the average magnitude of errors between predicted and actual values, without considering their direction. It is defined as:

$$\text{MAE} = \frac{1}{n} \sum_{t=1}^n |Y_t - \hat{Y}_t|,$$

1242 where:

1243

- 1244 •  $Y_t$  is the ground truth value at time step  $t$ ,
- 1245 •  $\hat{Y}_t$  is the predicted value at time step  $t$ ,
- 1246 •  $n$  is the total number of observations.

1247 MAE is scale-dependent and expresses the error in the same units as the data, making it directly  
1248 interpretable. It is robust to outliers compared to squared-error metrics, but does not penalize large  
1249 errors as heavily as MSE.

1250 **MSE** The *Mean Squared Error* (MSE) quantifies the average of the squared differences between  
1251 predicted and actual values. It is defined as:

$$1255 \quad 1256 \quad 1257 \quad \text{MSE} = \frac{1}{n} \sum_{t=1}^n (Y_t - \hat{Y}_t)^2,$$

1258 where:

1259

- 1260 •  $Y_t$  is the actual value at time  $t$ ,
- 1261 •  $\hat{Y}_t$  is the forecasted value at time  $t$ ,
- 1262 •  $n$  is the number of observations.

1263 MSE penalizes larger errors more severely due to the squaring operation, which makes it particularly  
1264 sensitive to outliers. Like MAE, MSE is also scale-dependent, and it is widely used in regression  
1265 and forecasting tasks due to its mathematical properties that facilitate optimization.

1266 **MAPE** MAPE is an evaluation metric used to measure the accuracy of forecasts in time series  
1267 analysis. It is defined as the mean of the absolute percentage differences between the actual values  
1268  $Y_t$  and the predicted values  $\hat{Y}_t$ . The formula for MAPE is:

$$1272 \quad 1273 \quad 1274 \quad \text{MAPE} = \frac{1}{n} \sum_{t=1}^n \left| \frac{Y_t - \hat{Y}_t}{Y_t} \right|,$$

1275 where:

1276

- 1277 •  $Y_t$  is the actual value at time  $t$ ,
- 1278 •  $\hat{Y}_t$  is the forecasted value at time  $t$ ,
- 1279 •  $n$  is the number of observations.

1280 This metric expresses the forecast error as a percentage of the actual values, making it scale-  
1281 independent and easy to interpret. However, it is sensitive to values of  $Y_t$  that are zero or close  
1282 to zero, as this can lead to division by zero or inflated error percentages.

1283 **CRPS** The *Continuous Ranked Probability Score* (CRPS) is a metric used in probabilistic forecasting  
1284 to evaluate the accuracy of predicted cumulative distribution functions (CDFs) against observed  
1285 values. Given a predicted distribution with CDF  $F$  and a ground truth value  $y$ , the CRPS is defined  
1286 as:

$$1290 \quad 1291 \quad 1292 \quad \text{CRPS}(F, y) = \int_0^1 2\Lambda_\alpha(F^{-1}(\alpha), y) d\alpha,$$

1293 where the quantile loss  $\Lambda_\alpha(q, y)$  is defined as:

$$1294 \quad \Lambda_\alpha(q, y) = (\alpha - \mathbf{1}\{y < q\})(y - q).$$

In practice, computing the CRPS integral can be computationally intensive. To address this, we approximate the CRPS using a discrete sum over a finite set of quantile levels. This approximation, often referred to as the mean weighted quantile loss (Park et al., 2022), is given by:

$$\text{CRPS} \approx \frac{1}{K} \sum_{k=1}^K \text{wQL}[\alpha_k],$$

where  $K$  is the number of quantile levels, and  $\{\alpha_1, \alpha_2, \dots, \alpha_K\}$  are the selected quantile levels (e.g.,  $\alpha_k = 0.1k$  for  $k = 1, 2, \dots, 9$  when  $K = 9$ ).

The weighted quantile loss  $\text{wQL}[\alpha]$  for each quantile level  $\alpha$  is calculated as:

$$\text{wQL}[\alpha] = 2 \frac{\sum_t \Lambda_\alpha(\hat{q}_t(\alpha), y_t)}{\sum_t |y_t|},$$

where:

- $\hat{q}_t(\alpha)$  is the predicted  $\alpha$ -quantile at time step  $t$ ,
- $y_t$  is the actual observed value at time  $t$ ,
- $\Lambda_\alpha(\hat{q}_t(\alpha), y_t)$  is the quantile loss at time  $t$  for quantile level  $\alpha$ .

## E FULL RESULTS

### E.1 ROBUSTNESS EVALUATION VIA ERROR BARS.

To evaluate the robustness of UniCA under different random seeds, we conduct experiments with seed values  $\{41, 42, 43, 44, 45\}$  on all uni-modal datasets and report the average performance along with 1-sigma standard deviation (mean  $\pm$  std), as shown in Table 7. Specifically, “C. (UniCA)” and “T. (UniCA)” denote the proposed UniCA framework built on top of Chronos Bolt and TimesFM, respectively.

The results demonstrate that UniCA consistently achieves strong performance with low variance across all metrics, indicating its robustness against random initialization. For example, on the GFC17 dataset, the MSE is  $0.096 \pm 0.003$  for Chronos-based UniCA and  $0.094 \pm 0.004$  for TimesFM-based UniCA, showcasing both accuracy and stability. This pattern holds across other datasets, supporting the statistical reliability and generalization ability of UniCA regardless of the underlying backbone.

Table 7: Error bar results of UniCA on uni-modal datasets. “C.” and “T.” indicate UniCA instantiated with Chronos-Bolt and TimesFM, respectively. All results are averaged over five runs with random seeds  $\{41, 42, 43, 44, 45\}$  and are reported as mean  $\pm$  standard deviation (1-sigma).

	Average	Bull	Cockatoo	COVID19	EPF	GFC12	GFC14	GFC17	Hog	M5	pdb	Retail	Spain	
C. (UniCA)	Average	0.457 $\pm$ 0.001	0.690 $\pm$ 0.004	0.822 $\pm$ 0.000	0.144 $\pm$ 0.000	0.434 $\pm$ 0.002	0.459 $\pm$ 0.010	0.319 $\pm$ 0.002	0.241 $\pm$ 0.004	0.716 $\pm$ 0.005	0.613 $\pm$ 0.001	0.190 $\pm$ 0.002	0.656 $\pm$ 0.007	0.196 $\pm$ 0.002
	MAE	0.509 $\pm$ 0.001	0.809 $\pm$ 0.002	0.874 $\pm$ 0.000	0.178 $\pm$ 0.000	0.440 $\pm$ 0.001	0.505 $\pm$ 0.012	0.361 $\pm$ 0.002	0.290 $\pm$ 0.005	0.781 $\pm$ 0.004	0.699 $\pm$ 0.002	0.228 $\pm$ 0.002	0.712 $\pm$ 0.005	0.230 $\pm$ 0.002
	MAPE	0.506 $\pm$ 0.002	0.639 $\pm$ 0.014	0.820 $\pm$ 0.002	0.179 $\pm$ 0.000	0.645 $\pm$ 0.004	0.559 $\pm$ 0.009	0.395 $\pm$ 0.002	0.286 $\pm$ 0.004	0.683 $\pm$ 0.005	0.764 $\pm$ 0.002	0.220 $\pm$ 0.002	0.655 $\pm$ 0.017	0.225 $\pm$ 0.002
	MSE	0.383 $\pm$ 0.002	0.700 $\pm$ 0.005	0.746 $\pm$ 0.000	0.041 $\pm$ 0.000	0.356 $\pm$ 0.002	0.285 $\pm$ 0.010	0.166 $\pm$ 0.002	0.096 $\pm$ 0.003	0.701 $\pm$ 0.006	0.566 $\pm$ 0.002	0.078 $\pm$ 0.001	0.769 $\pm$ 0.003	0.089 $\pm$ 0.001
T. (UniCA)	CRPS	0.429 $\pm$ 0.001	0.610 $\pm$ 0.002	0.848 $\pm$ 0.000	0.178 $\pm$ 0.000	0.293 $\pm$ 0.001	0.487 $\pm$ 0.010	0.354 $\pm$ 0.002	0.292 $\pm$ 0.002	0.700 $\pm$ 0.006	0.424 $\pm$ 0.001	0.232 $\pm$ 0.002	0.489 $\pm$ 0.004	0.239 $\pm$ 0.002
	Average	0.472 $\pm$ 0.001	0.730 $\pm$ 0.001	0.838 $\pm$ 0.001	0.143 $\pm$ 0.000	0.440 $\pm$ 0.002	0.468 $\pm$ 0.002	0.321 $\pm$ 0.002	0.237 $\pm$ 0.005	0.766 $\pm$ 0.003	0.612 $\pm$ 0.001	0.180 $\pm$ 0.002	0.655 $\pm$ 0.008	0.267 $\pm$ 0.008
	MAE	0.526 $\pm$ 0.001	0.876 $\pm$ 0.005	0.886 $\pm$ 0.001	0.178 $\pm$ 0.000	0.452 $\pm$ 0.001	0.512 $\pm$ 0.002	0.359 $\pm$ 0.002	0.285 $\pm$ 0.006	0.836 $\pm$ 0.003	0.701 $\pm$ 0.000	0.221 $\pm$ 0.002	0.709 $\pm$ 0.003	0.305 $\pm$ 0.009
	MAPE	0.514 $\pm$ 0.002	0.668 $\pm$ 0.011	0.812 $\pm$ 0.001	0.178 $\pm$ 0.000	0.643 $\pm$ 0.005	0.564 $\pm$ 0.002	0.402 $\pm$ 0.004	0.282 $\pm$ 0.005	0.726 $\pm$ 0.015	0.737 $\pm$ 0.002	0.210 $\pm$ 0.003	0.648 $\pm$ 0.027	0.296 $\pm$ 0.009
MSE	0.403 $\pm$ 0.001	0.757 $\pm$ 0.006	0.784 $\pm$ 0.001	0.040 $\pm$ 0.000	0.364 $\pm$ 0.001	0.299 $\pm$ 0.002	0.168 $\pm$ 0.001	0.094 $\pm$ 0.004	0.758 $\pm$ 0.006	0.587 $\pm$ 0.001	0.068 $\pm$ 0.001	0.776 $\pm$ 0.004	0.147 $\pm$ 0.007	
	CRPS	0.445 $\pm$ 0.001	0.655 $\pm$ 0.004	0.870 $\pm$ 0.001	0.177 $\pm$ 0.000	0.302 $\pm$ 0.001	0.499 $\pm$ 0.002	0.354 $\pm$ 0.001	0.287 $\pm$ 0.005	0.746 $\pm$ 0.005	0.426 $\pm$ 0.000	0.222 $\pm$ 0.002	0.485 $\pm$ 0.001	0.318 $\pm$ 0.009

### E.2 UNIMODAL FORECASTING

**Main results.** To provide a comprehensive comparison across all baseline and proposed methods, we report the detailed forecasting results on the 12 unimodal covariate-aware datasets in Table 8. This includes performance across four common evaluation metrics: MAE, MAPE, MSE, and CRPS. The models compared include traditional baselines (e.g., NBEATS, DeepAR, TFT), pretrained foundation models (e.g., TimesFM, Chronos), and our proposed adaptation strategies (UniCA, SFT, LR, ZS). We average each metric across all datasets and report both the raw values and metric-wise ranks.

To further illustrate the relative performance of each method, Figure 6 shows the average rank of each model across all datasets under each metric. Lower rank indicates better performance. As shown, our method **Chronos-Bolt (UniCA)** consistently outperforms all others in all four evaluation metrics. Notably, both Chronos and TimesFM, when adapted using UniCA, achieve significant improvements over their zero-shot and fine-tuned variants.

Table 8: Forecasting results on 12 unimodal covariate datasets.

		PatchTST	DeepAR	TFT	TIDE	NBEATsX	TimeXer	TTM	Moirai	TabPFN-TS	ChronosX	Chronos (Bolt)				TimesFM				Time-MoE	
												ZS	SFT	LR	UniCA	ZS	SFT	LR	UniCA	ZS	UniCA
Average		0.573	0.743	0.535	0.588	0.554	0.732	0.556	0.539	0.536	0.518	<b>0.472</b>	0.480	0.494	<b>0.457</b>	0.473	0.539	0.493	0.472	0.912	0.808
MAE		0.616	0.806	0.596	0.640	0.600	0.743	0.595	0.604	0.590	0.527	<b>0.521</b>	0.526	0.540	<b>0.509</b>	0.530	0.587	0.546	0.526	0.843	0.796
MAPE		0.633	0.718	0.596	0.649	0.608	0.738	0.592	0.593	0.600	0.580	0.522	0.514	0.569	<b>0.506</b>	0.523	0.598	0.557	0.514	0.946	0.938
MSE		0.531	0.726	0.449	0.525	0.482	0.752	0.440	0.462	0.467	0.471	0.403	0.418	0.413	<b>0.383</b>	0.402	0.466	0.405	0.403	0.971	0.643
CRPS		0.510	0.722	0.499	0.537	0.525	0.696	0.598	0.498	0.488	0.494	0.441	0.460	0.456	<b>0.429</b>	0.437	0.506	0.463	0.445	0.887	0.853
Average		0.758	0.796	0.794	0.795	0.797	0.849	0.783	<b>0.701</b>	0.776	0.782	0.722	0.719	0.716	<b>0.690</b>	0.716	0.723	0.715	0.739	0.892	0.848
MAE		0.871	0.924	0.902	0.881	0.886	0.948	0.869	0.857	0.874	0.862	0.835	0.828	0.815	<b>0.809</b>	0.842	0.837	0.831	0.876	0.968	0.923
MAPE		0.841	0.730	0.809	0.836	0.850	0.916	0.783	<b>0.609</b>	0.762	0.775	0.671	0.686	0.710	<b>0.639</b>	0.679	0.697	0.720	0.668	0.962	0.914
MSE		<b>0.693</b>	0.826	0.809	0.786	0.775	0.798	0.701	0.723	0.835	0.841	0.753	0.744	0.713	0.700	0.730	0.728	<b>0.696</b>	0.757	0.823	0.763
CRPS		0.629	0.705	0.656	0.676	0.677	0.734	0.775	0.616	0.634	0.650	0.628	0.622	<b>0.603</b>	0.610	0.611	0.631	0.613	0.655	0.814	0.790
Average		0.820	0.816	0.777	0.892	0.966	1.934	0.920	0.824	0.939	0.882	0.823	0.953	0.830	0.822	0.818	1.403	<b>0.805</b>	0.838	0.965	0.945
MAE		0.869	0.865	<b>0.827</b>	0.941	0.972	1.738	0.926	0.876	0.971	0.913	0.876	0.977	0.871	0.874	0.875	1.399	<b>0.852</b>	0.886	0.972	0.957
MAPE		0.836	0.853	0.800	0.861	0.906	1.498	0.815	0.831	0.936	0.864	0.803	0.867	0.795	0.820	0.803	1.364	<b>0.782</b>	0.812	0.891	0.874
MSE		0.741	0.732	<b>0.683</b>	0.850	1.002	2.835	0.822	0.761	0.931	0.826	0.755	0.927	0.774	0.746	0.769	1.440	<b>0.729</b>	0.784	0.905	0.879
CRPS		0.835	0.814	0.799	0.915	0.993	1.666	1.116	0.827	0.917	0.924	0.857	1.045	0.881	0.848	0.845	1.409	0.859	0.870	1.093	1.072
Average		0.221	0.186	0.324	0.219	0.272	0.235	0.231	0.264	0.166	0.144	<b>0.140</b>	0.170	0.144	0.143	0.169	0.168	0.143	0.730	0.764	
MAE		0.444	0.271	0.229	0.388	0.259	0.319	0.267	0.277	0.313	0.204	0.178	<b>0.170</b>	0.210	0.178	0.179	0.207	0.207	0.178	0.804	0.834
MAPE		0.458	0.277	0.229	0.398	0.257	0.315	0.266	0.272	0.311	0.205	<b>0.178</b>	<b>0.172</b>	0.212	0.179	0.179	0.207	0.208	0.178	0.804	0.843
MSE		0.191	0.078	0.061	0.146	0.092	0.131	0.082	0.104	0.142	0.054	0.041	<b>0.058</b>	0.052	0.041	0.040	0.048	0.052	0.040	0.564	0.594
CRPS		0.414	0.258	0.225	0.367	0.267	0.323	0.325	0.270	0.291	0.202	0.180	0.177	0.205	0.178	<b>0.174</b>	0.213	0.204	0.177	0.750	0.785
Avg		0.506	0.638	0.542	0.577	0.489	0.626	0.539	0.574	0.528	0.577	0.465	<b>0.423</b>	0.450	0.434	0.449	0.465	0.436	0.440	0.762	0.767
MAE		0.526	0.875	0.574	0.622	0.514	0.663	0.546	0.626	0.541	0.499	0.461	0.442	0.469	<b>0.440</b>	0.459	0.487	0.468	0.452	0.826	0.826
MAPE		0.740	<b>0.534</b>	0.750	0.797	0.688	0.897	0.779	0.772	0.808	0.705	0.725	0.597	0.654	0.645	0.657	0.655	<b>0.589</b>	0.643	1.007	1.031
MSE		0.413	0.554	0.466	0.476	0.407	0.507	0.416	0.482	0.412	0.771	0.365	0.357	0.366	<b>0.356</b>	0.378	0.397	0.376	0.364	0.623	0.613
CRPS		0.345	0.589	0.377	0.412	0.346	0.439	0.415	0.418	0.352	0.335	0.307	0.295	0.309	<b>0.293</b>	0.300	0.320	0.311	0.302	0.594	0.596
Average		0.522	0.817	0.648	0.568	0.511	0.571	0.578	0.521	0.534	0.501	0.479	0.469	0.509	<b>0.459</b>	0.476	0.490	0.537	<b>0.468</b>	0.815	0.818
MAE		0.574	0.880	0.694	0.620	0.559	0.625	0.591	0.571	0.585	0.546	0.525	<b>0.510</b>	0.548	<b>0.505</b>	0.523	0.535	0.532	0.512	0.838	0.841
MAPE		0.616	0.751	0.764	0.661	0.601	0.649	0.640	0.624	0.619	0.595	0.576	0.560	<b>0.987</b>	<b>0.559</b>	0.575	0.601	0.676	0.872	0.881	
MSE		0.345	0.729	0.471	0.391	0.327	0.396	0.368	0.346	0.375	0.335	0.306	0.302	0.323	<b>0.285</b>	0.311	0.304	0.317	<b>0.299</b>	0.670	0.670
CRPS		0.551	0.908	0.654	0.600	0.557	0.613	0.715	0.543	0.558	0.526	0.511	0.502	0.536	<b>0.487</b>	0.497	0.519	0.529	0.499	0.879	0.882
Average		0.349	1.279	0.361	0.376	0.324	<b>0.268</b>	0.398	0.362	0.361	0.339	0.331	0.324	0.344	0.319	0.320	0.330	0.337	0.321	0.707	0.727
MAE		0.391	1.205	0.405	0.421	0.364	0.325	0.438	0.413	0.403	0.368	0.363	0.385	0.361	0.368	0.375	0.359	<b>0.059</b>	0.059	0.059	0.059
MAPE		0.446	1.201	0.449	0.454	0.405	<b>0.313</b>	0.497	0.440	0.449	0.401	0.411	0.409	0.428	0.395	0.401	0.423	0.425	0.402	1.463	1.485
MSE		0.181	1.204	0.198	0.212	0.168	0.215	0.222	0.195	0.202	0.170	0.177	0.169	0.186	0.166	0.168	0.168	0.168	0.168	0.004	0.004
CRPS		0.376	1.434	0.393	0.417	0.361	<b>0.320</b>	0.434	0.397	0.392	0.368	0.367	0.364	0.378	0.354	0.351	0.362	0.368	0.354	1.303	1.359
Average		0.288	0.809	0.320	0.312	0.286	0.340	0.303	0.302	0.284	0.251	0.240	0.238	0.270	0.241	0.242	0.274	0.262	<b>0.237</b>	0.772	0.758
MAE		0.346	0.856	0.377	0.369	0.339	0.402	0.338	0.363	0.341	0.299	0.287	<b>0.283</b>	0.319	0.290	0.295	0.328	0.312	<b>0.285</b>	0.817	0.801
MAPE		0.346	0.820	0.374	0.372	0.337	0.392	0.326	0.351	0.330	0.297	0.284	<b>0.280</b>	0.321	0.286	0.289	0.324	0.309	<b>0.282</b>	0.815	0.813
MSE		0.124	0.623	0.155	0.144	0.127	0.172	0.125	0.141	0.131	0.104	0.097	<b>0.092</b>	0.115	0.096	0.097	0.116	0.106	<b>0.094</b>	0.601	0.590
CRPS		0.337	0.938	0.372	0.362	0.343	0.393	0.421	0.355	0.334	0.302	0.293	0.289	0.328	0.322	0.322	0.328	0.322	<b>0.287</b>	0.854	0.826
Average		0.790	1.553	0.839	0.837	0.886	1.792	0.916	0.873	0.835	0.807	0.771	0.798	<b>0.810</b>	<b>0.760</b>	0.828	0.802	0.766	1.241	0.967	
MAE		0.856	1.518	0.893	0.891	0.914	1.480	0.933	0.951	0.897	0.872	0.838	0.853	0.889	<b>0.781</b>	0.836	0.880	0.868	<b>0.836</b>	1.203	0.976
MAPE		0.786	1.173	0.859	0.868	0.906	1.547	0.814	0.806	0.839	0.706	<b>0.689</b>	0.708	<b>0.683</b>	0.724	0.814	0.789	0.726	1.012	1.024	
MSE		0.767	2.209	0.822	0.807	0.863	2.145	0.902	0.920	0.824	0.864	0.808	0.853	0.817	<b>0.701</b>	0.757	0.814	0.771	0.758	1.554	0.890
CRPS		0.751	1.311	0.784	0.782	0.835	1.994	1.015	0.816	0.781	0.785	0.750	0.782	0.794	<b>0.700</b>	0.723	0.803	0.781	0.746	1.195	0.980
Avg		1.127	0.692	0.624	0.903	0.646	0.629	0.724	0.680	0.663	0.632	<b>0.600</b>	0.629	0.613	0.608	0.629	0.609	0.613	0.739	0.707	
MAE		1.033	0.746	0.728	0.911	1.000	0.745	0.776	0.793	0.759	0.746	0.710	<b>0.690</b>	0.711	0.699						

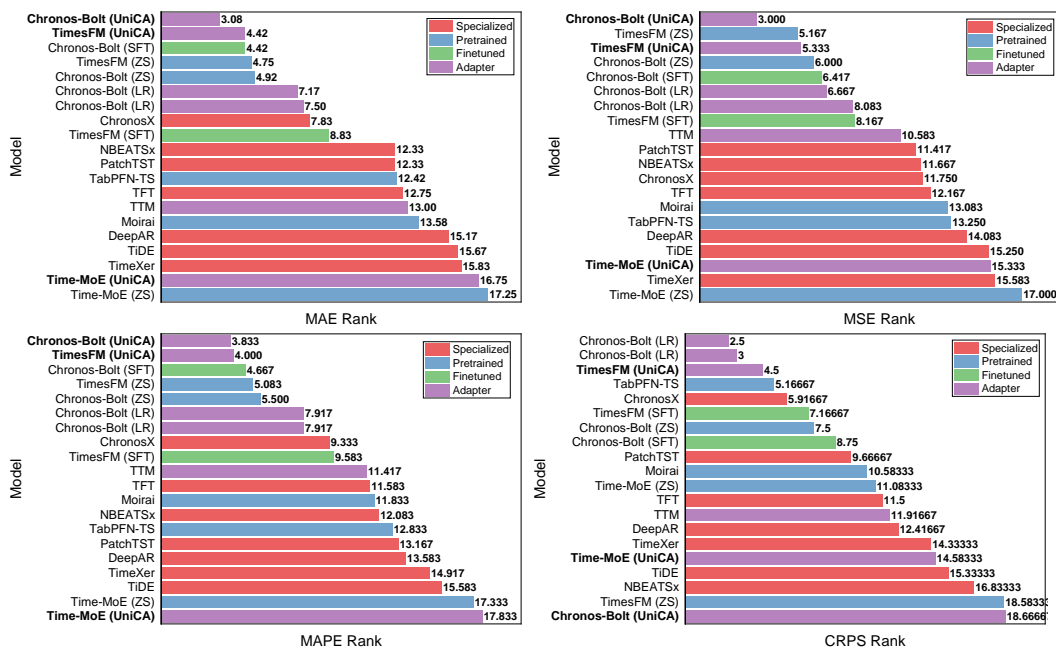


Figure 6: Metrics rank on uni-modal covariate-aware datasets.

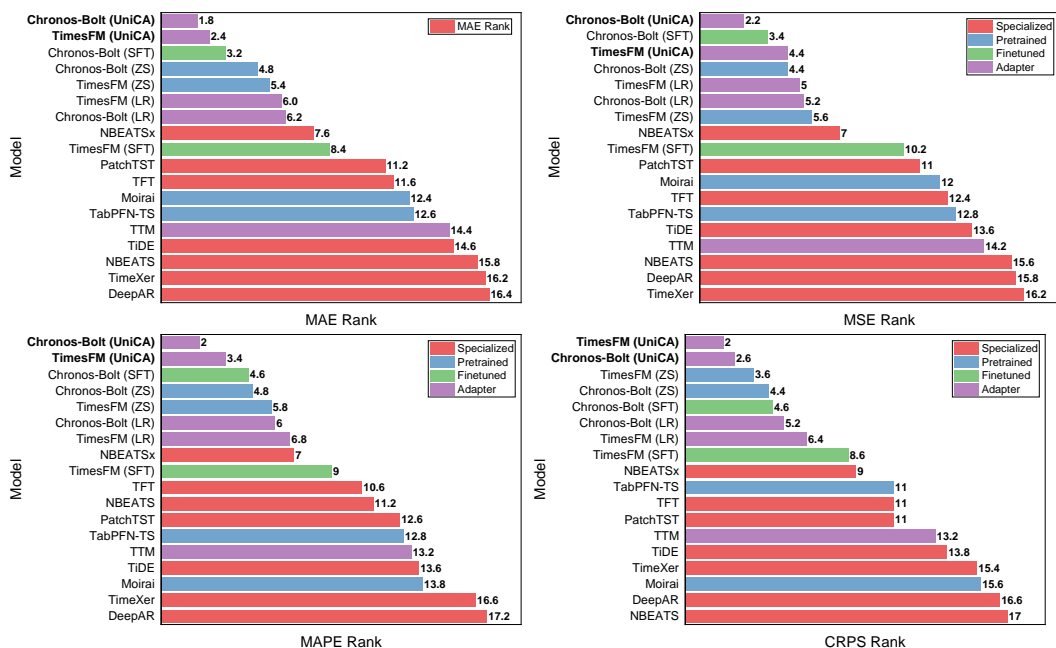


Figure 7: Metrics rank on EPF subsets.

1458 Table 9: Forecasting results on subsets of EPF.  
1459

		PatchTST	NBEATS	DeepAR	TFT	Tide	NBEATSx	TimeXer	Moirai	TTM	TabPFN-TS	Chronos-Bolt				TimesFM				
												ZS	SFT	LR	UniCA	ZS	SFT	LR	UniCA	
1460	Average	0.497	0.653	0.666	0.482	0.514	0.438	0.576	0.517	0.510	0.496	0.419	0.410	0.420	<b>0.399</b>	0.415	0.450	0.414	0.405	
		MAE	0.559	0.759	0.771	0.543	0.590	0.496	0.647	0.596	0.558	0.555	0.467	0.456	0.477	<b>0.450</b>	0.467	0.509	0.471	0.458
		MAPE	0.598	0.564	0.780	0.563	0.600	0.519	0.698	0.594	0.600	0.591	0.507	0.495	0.498	<b>0.476</b>	0.500	0.532	0.489	<b>0.487</b>
		MSE	0.413	0.594	0.535	0.422	0.426	0.356	0.481	0.444	0.407	0.427	0.349	0.337	0.348	<b>0.329</b>	0.348	0.383	0.342	0.338
		CRPS	0.417	0.692	0.579	0.399	0.441	0.380	0.476	0.436	0.476	0.411	0.354	0.351	0.357	<b>0.341</b>	0.346	0.377	0.355	<b>0.339</b>
1464	BE	Average	0.416	0.570	0.623	0.432	0.484	0.420	0.546	0.458	0.440	0.410	0.357	0.357	0.358	<b>0.356</b>	0.363	0.407	0.365	<b>0.356</b>
		MAE	0.518	0.704	0.819	0.536	0.605	0.526	0.681	0.574	0.546	0.519	0.452	0.451	0.453	0.451	0.457	0.513	0.456	<b>0.450</b>
		MAPE	0.488	0.640	0.724	0.461	0.572	0.482	0.669	0.520	0.497	0.479	0.399	0.399	0.399	0.391	0.398	0.430	0.400	<b>0.391</b>
		MSE	0.417	0.538	0.558	0.478	0.479	0.416	0.511	0.472	0.420	0.400	<b>0.362</b>	0.363	0.365	0.366	0.385	0.439	0.386	0.374
		CRPS	0.242	0.401	0.390	0.254	0.282	0.257	0.323	0.267	0.298	0.242	0.214	0.216	<b>0.213</b>	0.213	0.245	0.217	<b>0.210</b>	
1466	DE	Average	0.637	0.940	0.652	0.638	0.650	0.567	0.734	0.631	0.680	0.686	0.620	0.556	0.575	0.544	0.555	0.575	<b>0.518</b>	<b>0.534</b>
		MAE	0.630	1.124	0.648	0.649	0.690	0.589	0.727	0.669	0.650	0.679	0.604	0.557	0.592	0.567	0.587	0.557	<b>0.553</b>	
		MAPE	0.861	<b>0.276</b>	0.862	0.836	0.776	0.706	0.948	0.754	0.875	0.916	0.832	0.735	0.724	0.702	0.740	0.751	<b>0.633</b>	0.701
		MSE	0.485	1.104	0.490	0.485	0.498	0.407	0.593	0.504	0.499	0.540	0.487	0.406	0.435	0.404	0.405	0.428	<b>0.366</b>	0.385
		CRPS	0.574	1.257	0.609	0.581	0.635	0.566	0.665	0.599	0.696	0.609	0.559	0.527	0.551	0.516	0.510	0.534	0.517	<b>0.497</b>
1469	FR	Average	0.421	0.808	0.575	0.473	0.499	0.414	0.564	0.493	0.456	0.425	<b>0.349</b>	0.351	0.361	<b>0.350</b>	0.364	0.407	0.374	0.359
		MAE	0.488	0.937	0.672	0.539	0.582	0.472	0.661	0.576	0.521	0.493	0.398	<b>0.392</b>	0.412	0.394	0.412	0.464	0.426	0.408
		MAPE	0.450	0.853	0.724	0.485	0.548	0.440	0.634	0.533	0.472	0.468	0.360	<b>0.356</b>	0.371	<b>0.352</b>	0.366	0.409	0.378	0.362
		MSE	0.421	0.676	0.450	0.515	0.476	0.417	0.521	0.482	0.426	0.410	<b>0.366</b>	0.387	0.385	0.384	0.403	0.441	0.405	0.394
		CRPS	0.325	0.765	0.451	0.355	0.388	0.327	0.441	0.381	0.403	0.328	<b>0.270</b>	0.271	0.275	0.271	0.276	0.314	0.288	0.273
1472	NP	Average	0.704	0.570	0.809	0.543	0.602	0.498	0.641	0.679	0.644	0.632	0.489	0.507	0.529	<b>0.476</b>	0.517	0.564	0.531	0.501
		MAE	0.776	0.588	0.912	0.581	0.650	0.528	0.682	0.749	0.670	0.673	0.523	0.529	0.572	<b>0.506</b>	0.546	0.604	0.555	0.528
		MAPE	0.828	0.653	0.892	0.661	0.709	0.624	0.781	0.794	0.771	0.716	<b>0.612</b>	0.653	0.662	0.614	0.665	0.707	0.689	0.648
		MSE	0.556	0.418	0.642	0.430	0.463	0.367	0.514	0.552	0.496	0.569	0.364	0.374	0.396	<b>0.341</b>	0.387	0.431	0.397	0.375
		CRPS	0.656	0.622	0.792	0.500	0.586	0.474	0.587	0.625	0.638	0.570	0.455	0.472	0.482	<b>0.445</b>	0.469	0.513	0.482	<b>0.452</b>
1474	PIM	Average	0.305	0.374	0.672	0.322	0.335	0.289	0.393	0.325	0.331	0.326	0.281	0.277	0.278	<b>0.268</b>	0.277	0.299	0.283	0.277
		MAE	0.386	0.444	0.804	0.409	0.421	0.363	0.485	0.412	0.401	0.410	0.355	0.353	0.354	<b>0.340</b>	0.352	0.378	0.360	0.352
		MAPE	0.363	0.401	0.697	0.371	0.397	0.344	0.459	0.373	0.385	0.373	0.332	0.330	0.337	<b>0.321</b>	0.333	0.363	0.345	0.333
		MSE	0.184	0.235	0.537	0.204	0.210	0.172	0.265	0.210	0.195	0.215	0.166	0.156	0.157	<b>0.150</b>	0.162	0.175	0.156	0.162
		CRPS	0.286	0.415	0.651	0.305	0.313	0.278	0.363	0.306	0.345	0.305	0.271	0.268	0.265	<b>0.260</b>	0.262	0.279	0.272	<b>0.262</b>

## 1476 E.3 MULTI-MODAL FORECASTING

## 1477

1478 **Time-MMD (TS-Text).** Table 10 reports the full forecasting results on the Time-MMD benchmark across seven domains: *Climate*, *Energy*, *Environment*, *Health*, *Security*, *SocialGood*, and *Traffic*. We compare UniCA with strong baselines, including classic models (e.g., DeepAR, TFT), recent pretrained models (e.g., Chronos-Bolt, TimesFM), and domain-specific models (e.g., Time-LLM, TTM, Moirai). Metrics include Mean Absolute Error (MAE), Mean Absolute Percentage Error (MAPE), Mean Squared Error (MSE), and Continuous Ranked Probability Score (CRPS).

1487 UniCA consistently achieves the best or competitive performance across most domains and metrics, demonstrating its versatility and scalability in handling heterogeneous covariates under diverse multimodal forecasting scenarios.

1492 Table 10: Full forecasting results on Time-MMD.

## 1493

		NBEATSx	PatchTST	DeepAR	TFT	TFT(+CH)	TIDE	TIDE(+CH)	Time-LLM	TTM	Moirai	TabPFN-TS	MM-TSP	ChatTime	Chronos (Bolt)				TimesFM			
															ZS	SFT	LR	UniCA	ZS	SFT	LR	UniCA
1495	Climate	Average	0.840	0.894	1.270	0.971	0.934	0.920	0.889	0.818	0.778	0.742	0.801	0.691	1.213	0.892	0.748	0.774	0.647	0.737	0.794	0.703
		MAE	0.884	1.009	1.219	0.958	0.928	0.976	0.847	0.846	0.821	0.837	0.777	0.647	<b>0.647</b>	0.737	0.794	0.716	0.869	0.703	0.918	0.818
		MAPE	0.717	0.778	0.998	1.042	1.035	0.900	0.856	0.766	0.651	0.715	0.655	2.227	0.674	0.721	0.634	0.646	0.776	0.601	0.648	0.634
		MSE	0.782	0.793	1.605	0.992	0.885	0.869	0.813	0.723	0.685	0.699	0.787	0.618	1.361	0.637	0.647	0.614	0.608	0.732	0.607	0.769
		CRPS	0.980	0.996	1.260	0.891	0.886	0.937	0.932	0.935	0.909	0.735	0.762	0.727	0.618	<b>0.618</b>	0.681	0.799	0.693	0.640	0.841	0.645
1497	Energy	Average	0.628	0.720	0.815	0.708	0.800	0.573	0.578	0.599	0.536	0.545	0.536	0.509	1.799	<b>0.505</b>	0.626	0.515	0.529	0.532	0.555	0.559
		MAE	0.712	0.788	0.779	0.988	0.685	0.682	0.687	0.635	0.705	0.638	0.635	1.000	<b>0.622</b>	0.685	0.624	0.635	0.630	0.635	0.714	0.714
		MAPE	0.510	0.710	1.048	0.744	0.718	0.569	0.589	0.498	0.566	0.393	0.563	0.406	1.361	0.462	0.682	0.462	0.541	0.542	<b>0.255</b>	0.259
		MSE	0.519	0.626	0.706	0.599	0.641	0.541	0.547	0.546	0.547	0.541	0.547	0.541	1.718	0.484	0.586	0.481	0.586	0.587	0.615	0.615
		CRPS	0.721	0.665	0.770	0.676	0.778	0.773	0.774	0.775	0.776	0.777	0.777	0.777	1.742	<b>0.528</b>	0.740	0.779	0.728	0.753	0.799	0.756
1500	Health	Average	0.721	0.665	0.770	0.676	0.646	0.667	0.733	0.733	0.733</											

1512 Table 11: Forecasting performance on MMSP (TS-Image multimodal) dataset.  
1513

	PTST	NBS	D.AR	TFT	TFT (+CH)	TIDE	TIDE (+CH)	TTM	Moirai	PFN	ESF	MM-TSF	Chronos (Bolt)			TimesFM			Time-MOE		
													ZS	SFT	UniCA	ZS	SFT	UniCA	ZS	UniCA	
MMSP	<b>Average</b>	0.485	0.152	0.137	<b>0.112</b>	<b>0.103</b>	0.292	0.135	0.408	0.238	0.555	0.378	0.127	0.120	0.140	0.121	0.158	0.167	0.147	0.703	0.607
	MAE	0.682	0.219	0.216	<b>0.177</b>	<b>0.168</b>	0.438	0.206	0.263	0.378	0.711	0.566	0.200	0.193	0.225	0.193	0.245	0.258	0.229	0.814	0.765
	MAPE	0.020	0.030	0.019	0.034	0.021	0.022	<b>0.014</b>	0.090	0.038	0.187	<b>0.016</b>	0.037	0.019	0.023	0.019	0.049	0.080	0.046	0.755	0.337
	MSE	0.662	0.107	0.097	<b>0.067</b>	<b>0.067</b>	0.297	0.100	0.095	0.206	0.633	0.478	0.090	0.090	0.099	0.090	0.113	0.100	0.098	0.538	0.653
	CRPS	0.576	0.252	0.214	<b>0.168</b>	<b>0.157</b>	0.410	0.220	1.183	0.329	0.691	0.452	0.183	0.180	0.212	0.180	0.227	0.231	0.215	0.707	0.672

1518  
1519 E.4 IMPUTATION  
15201521 UniCA is a general covariate adaptation framework for time-series foundation models (TSFMs). Its  
1522 applicability is therefore not limited to forecasting—UniCA can be attached to any downstream task  
1523 that the underlying TSFM supports, provided the task is covariate-aware.1524 To demonstrate this, we evaluate UniCA on the *imputation* setting of the MOMENT  
1525 TSFM Goswami et al. (2024), which natively supports forecasting, classification, anomaly detec-  
1526 tion, and imputation. Among these tasks, only imputation naturally involves multivariate inputs or  
1527 covariates, making it the most appropriate benchmark for UniCA.1528 For each dataset (ETTh1, ETTh2, ETTm1, ETTm2, Electricity, Weather), we treat the OT column  
1529 as the target variable and use all remaining variables as past dynamic real covariates. Each dataset is  
1530 split with a 6:2:2 ratio. Following the MOMENT imputation setup, on the test split we extract slid-  
1531 ing windows of length 512 and randomly mask patches of length 8 using MOMENT’s patch-based  
1532 masking module at mask ratios 12.5%, 25%, 37.5%, 50%. MOMENT is loaded in “reconstruc-  
1533 tion” mode and is never fine-tuned; its RevIN normalizer and reconstruction head remain fixed  
1534 throughout.1535 UniCA operates on top of the frozen MOMENT encoder: the target context is tokenized by MO-  
1536 MENT; all covariates are homogenized and fused through UniCA’s gated residual and attention  
1537 modules; and the fused representation is passed directly into MOMENT’s frozen reconstruction  
1538 head. During training, we optimize *only* UniCA’s parameters to minimize squared error on the  
1539 masked target positions. MOMENT’s weights remain completely frozen. At evaluation time, we  
1540 compare zero-shot MOMENT and MOMENT+UniCA using the same patch masks and report MSE  
1541 and MAE over the masked entries only. Results are shown in Table 12.1542 Across all six datasets and all four mask ratios, UniCA consistently improves imputation over  
1543 zero-shot MOMENT model. Averaged over mask ratios, UniCA reduces MSE by roughly 33–35%  
1544 on ETTh1/ETTh2, about 60–85% on ETTm1/ETTm2, 45% on electricity, and 40% on weather,  
1545 with corresponding MAE reductions of about 20–25% (ETTh), 40–65% (ETTm), 25% (electric-  
1546 ty), and 23% (weather). The gains are monotonic in the mask ratio: UniCA’s relative improvement  
1547 is smallest at 12.5% masking and largest at 50% masking on every dataset, showing that covariate-  
1548 aware adaptation becomes increasingly beneficial as the imputation problem becomes harder.1549 F SHOWCASES  
15501552 In this section, we present a detailed case study to demonstrate the effectiveness of our proposed  
1553 UniCA framework. We analyze the feature attention affinity, important covariates identified by our  
1554 model, and compare the prediction performance with and without UniCA adaptation.1556 Figure 8, 9, 10, 11 illustrate our analysis on two time series samples for each dataset, labeled as (a)  
1557 and (b). The visualization is organized into three components for each sample: Important Features  
1558 Visualization (top), Prediction Comparison (middle), and Feature Weights Visualization (bottom).  
1559 The Important Features Visualization reveals how our model identifies and leverages key covari-  
1560 ates during prediction. In figure 8 (a), covariate 18 demonstrates high importance (0.8323) while  
1561 covariate 7 shows minimal contribution (0.0125). Similarly, in sample (b), covariate 18 maintains  
1562 high importance (0.8586) while covariate 24 has low importance (0.0077). This selective attention  
1563 mechanism enables UniCA to focus on the most relevant covariates for each specific forecasting  
1564 task, effectively filtering out noise from less informative features.1565 The Prediction Comparison clearly demonstrates the superior performance of UniCA-adapted mod-  
1566 els compared to their non-adapted counterparts. The middle rows show predictions without UniCA

1566  
 1567  
 1568  
 1569  
 1570  
 1571  
 1572  
 1573  
 1574  
 1575  
 1576  
 1577  
 1578  
 1579  
 1580  
 1581

Table 12: Imputation performance of zero-shot MOMENT and UniCA-adapted MOMENT on six ETT/electricity/weather benchmarks under four random patch-masking ratios (12.5%, 25%, 37.5%, 50%). Reported metrics are MSE and MAE on the masked target entries, together with percentage-point improvements of UniCA over the MOMENT baseline (negative values indicate lower error with UniCA).

1582  
 1583  
 1584  
 1585  
 1586  
 1587  
 1588  
 1589  
 1590  
 1591  
 1592  
 1593  
 1594  
 1595  
 1596  
 1597  
 1598  
 1599  
 1600  
 1601  
 1602  
 1603  
 1604  
 1605  
 1606  
 1607  
 1608  
 1609  
 1610  
 1611  
 1612  
 1613  
 1614  
 1615  
 1616  
 1617  
 1618  
 1619

Dataset	Mask Ratio	MSE			MAE		
		MOMENT	UniCA	Improve	MOMENT	UniCA	Improve
ETTh1	12.5%	0.016	<b>0.012</b>	-23.9%	0.093	<b>0.079</b>	-14.5%
	25.0%	0.022	<b>0.016</b>	-27.9%	0.110	<b>0.090</b>	-18.4%
	37.5%	0.030	<b>0.019</b>	-35.4%	0.128	<b>0.100</b>	-21.6%
	50.0%	0.041	<b>0.025</b>	-38.3%	0.152	<b>0.115</b>	-24.4%
	Average	0.027	<b>0.018</b>	-33.3%	0.121	<b>0.096</b>	-20.4%
ETTh2	12.5%	0.042	<b>0.026</b>	-37.8%	0.150	<b>0.108</b>	-27.6%
	25.0%	0.059	<b>0.039</b>	-33.8%	0.176	<b>0.128</b>	-27.3%
	37.5%	0.086	<b>0.059</b>	-31.8%	0.212	<b>0.154</b>	-27.0%
	50.0%	0.131	<b>0.084</b>	-35.5%	0.269	<b>0.188</b>	-30.2%
	Average	0.079	<b>0.052</b>	-34.5%	0.202	<b>0.145</b>	-28.2%
ETTm1	12.5%	0.007	0.003	-48.4%	0.057	<b>0.039</b>	-31.3%
	25.0%	0.010	<b>0.004</b>	-58.0%	0.068	<b>0.043</b>	-37.5%
	37.5%	0.015	<b>0.005</b>	-62.9%	0.083	<b>0.048</b>	-42.1%
	50.0%	0.021	<b>0.007</b>	-65.4%	0.102	<b>0.056</b>	-45.4%
	Average	0.013	<b>0.005</b>	-61.1%	0.077	<b>0.046</b>	-40.2%
ETTm2	12.5%	0.015	<b>0.002</b>	-83.1%	0.080	<b>0.032</b>	-59.6%
	25.0%	0.028	<b>0.004</b>	-85.0%	0.108	<b>0.040</b>	-63.0%
	37.5%	0.051	<b>0.007</b>	-86.2%	0.148	<b>0.051</b>	-65.6%
	50.0%	0.082	<b>0.014</b>	-83.3%	0.195	<b>0.068</b>	-65.0%
	Average	0.044	<b>0.007</b>	-84.4%	0.133	<b>0.048</b>	-63.9%
electricity	12.5%	0.124	<b>0.098</b>	-20.6%	0.258	<b>0.234</b>	-9.3%
	25.0%	0.159	<b>0.110</b>	-30.4%	0.290	<b>0.248</b>	-14.4%
	37.5%	0.232	<b>0.127</b>	-45.2%	0.351	<b>0.266</b>	-24.2%
	50.0%	0.376	<b>0.151</b>	-59.9%	0.458	<b>0.288</b>	-37.0%
	Average	0.223	<b>0.122</b>	-45.4%	0.339	<b>0.259</b>	-23.6%
weather	12.5%	0.000	<b>0.000</b>	-19.5%	0.008	<b>0.007</b>	-10.6%
	25.0%	0.000	<b>0.000</b>	-35.0%	0.009	<b>0.008</b>	-19.4%
	37.5%	0.000	<b>0.000</b>	-43.9%	0.012	<b>0.008</b>	-26.8%
	50.0%	0.000	<b>0.000</b>	-45.2%	0.014	<b>0.010</b>	-30.2%
	Average	0.000	<b>0.000</b>	-39.5%	0.011	<b>0.008</b>	-23.3%

adaptation, while the lower rows display predictions with UniCA adaptation. Both models generate prediction intervals (10%-90%), but the UniCA-adapted model produces forecasts that align more closely with the ground truth values. Notably, the predictions with UniCA show better alignment with the temporal patterns and magnitude of the ground truth, particularly in the forecast horizon (the shaded area after the vertical dotted line).

The Feature Weights Visualization at the bottom provides insight into how attention is distributed across different feature dimensions and sequence positions. The heatmaps reveal that certain feature dimensions consistently receive higher attention weights (shown in brighter yellow), indicating their greater influence on the final prediction. These patterns vary between samples (a) and (b), highlighting UniCA’s ability to adapt dynamically to different time series characteristics.

Our case study demonstrates that UniCA effectively identifies important covariates through its attention mechanism and significantly improves prediction accuracy by incorporating this covariate information. The comparison between adapted and non-adapted models confirms that UniCA successfully bridges TSFMs with covariate-aware forecasting while preserving the foundation model’s generalization capabilities. Furthermore, the feature weight visualizations provide interpretability insights, showing which dimensions and temporal positions are most influential for specific forecasting tasks.

## G MORE ABLATION

### G.1 FUSION POSITION.

To further understand the impact of fusion positions in integrating covariate information, we conduct an ablation study by varying where the past and future covariates are fused within the TSFM pipeline. Specifically, we compare four fusion strategies: Pre-Pre, Post-Pre, Post-Post, and Pre-Post (our default setting). These denote whether past and future covariates are fused before (Pre) or after (Post) the temporal encoder.

As shown in Figure 12, the results indicate that the choice of fusion position has a relatively minor impact on the overall forecasting performance. On TimesFM, all variants achieve similar performance, with the aggregated error ranging from 0.472 to 0.476. Interestingly, although Post-Post slightly underperforms the others, the differences remain marginal. On Chronos-Bolt, all configurations perform nearly identically, with Post-Post achieving the lowest error (0.455), reinforcing the robustness of our fusion design. These findings suggest that while the timing of fusion can affect the model’s attention mechanism and how it contextualizes covariate information, UniCA remains stable and effective regardless of specific fusion positions. This reflects the flexibility of our attention-based fusion modules and their adaptability across model architectures.

### G.2 INFLUENCE OF MODALITY ENCODER

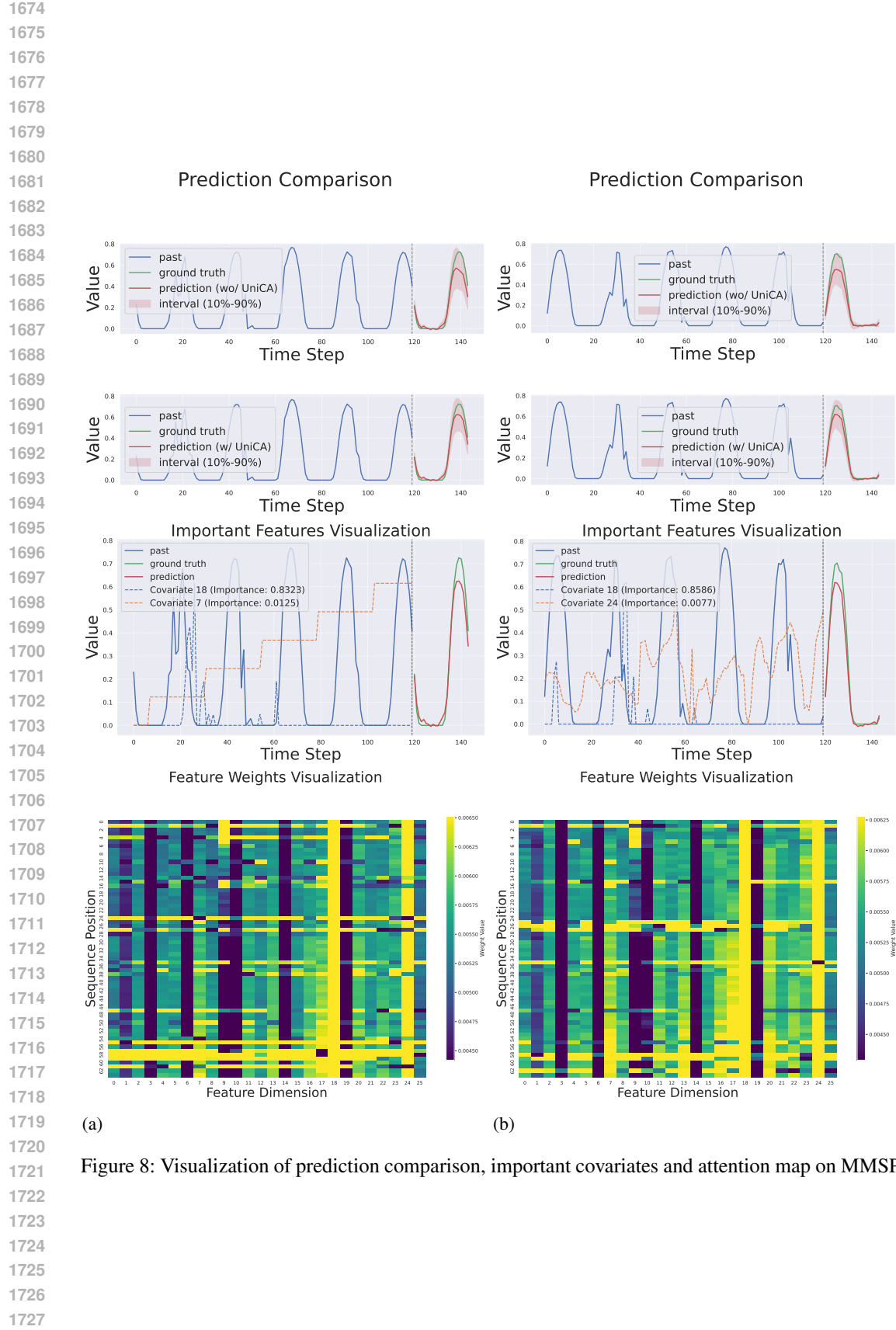
To investigate the effect of different text modality encoders on forecasting performance, we conduct a comprehensive evaluation on the Time-MMD benchmark across six domains: *Climate*, *Energy*, *Environment*, *Health*, *Security*, and *SocialGood*. We embed the same textual covariates using four representative pretrained language models—GIST (Solatorio, 2024)<sup>10</sup> (a text embedding model), BERT (Devlin et al., 2019)<sup>11</sup>, GPT-2 (Radford et al., 2019)<sup>12</sup>, and LLAMA-2 (Touvron et al., 2023)<sup>13</sup>—and report forecasting results under two forecasting backbones: Chronos-Bolt and TimesFM, both implemented via the UniCA framework. The results are summarized in Table 13. Chronos consistently benefits from text embeddings, with minor variation across encoder types. In contrast, TimesFM exhibits significantly larger fluctuations in performance depending on the encoder. For instance, under the *Environment* domain, the MAE of TimesFM ranges from 0.756 (GIST) to 1.181 (BERT), whereas Chronos maintains stable performance across all encoders (MAE = 0.738 for all). Among all text encoders, GIST demonstrates the most consistent performance across both Chronos and TimesFM, achieving the lowest average forecasting errors in domains such as *Security*

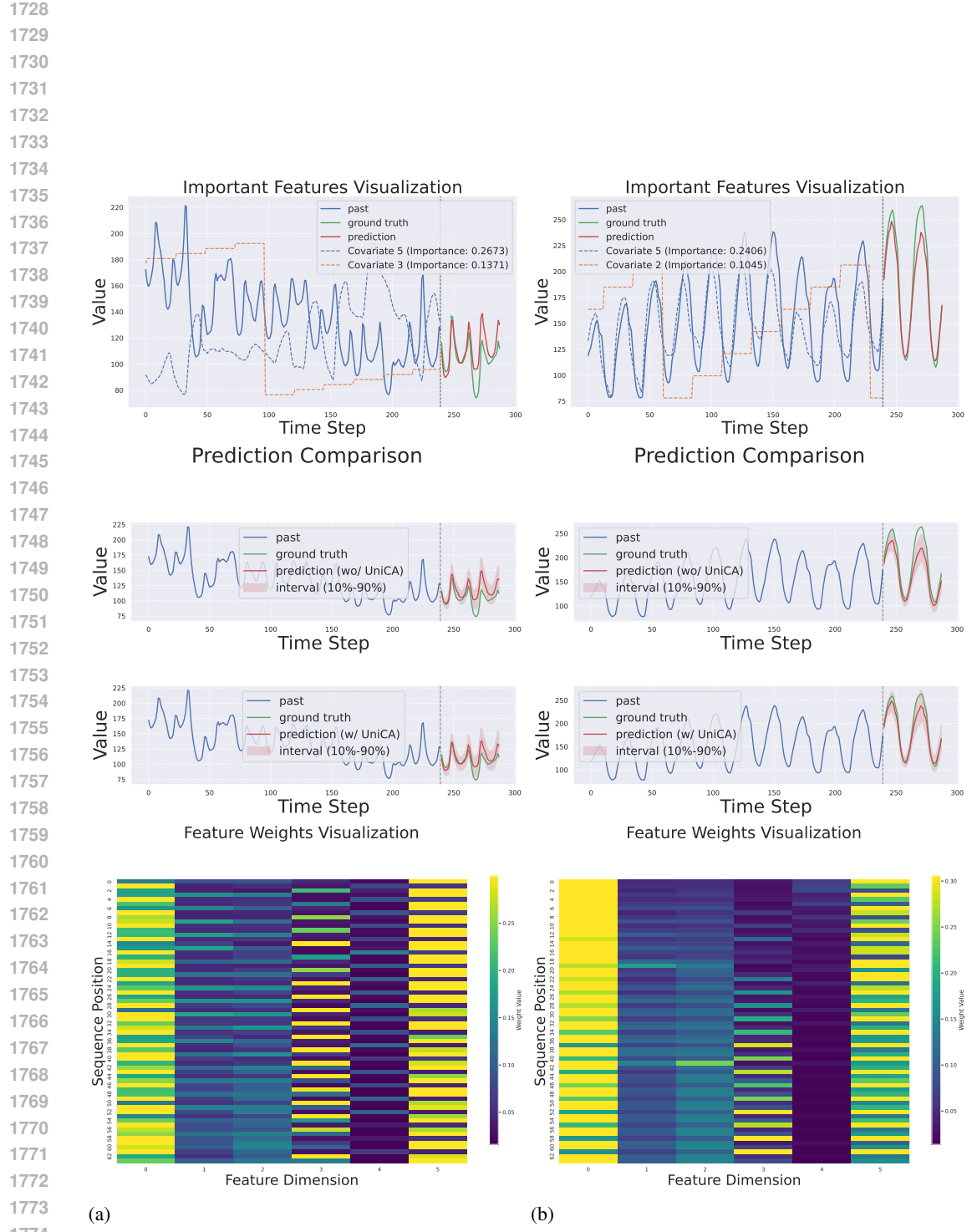
<sup>10</sup><https://huggingface.co/avsolatorio/GIST-small-Embedding-v0>

<sup>11</sup><https://huggingface.co/google-bert/bert-base-uncased>

<sup>12</sup><https://huggingface.co/openai-community/gpt2>

<sup>13</sup><https://huggingface.co/meta-llama/Llama-2-7b-hf>





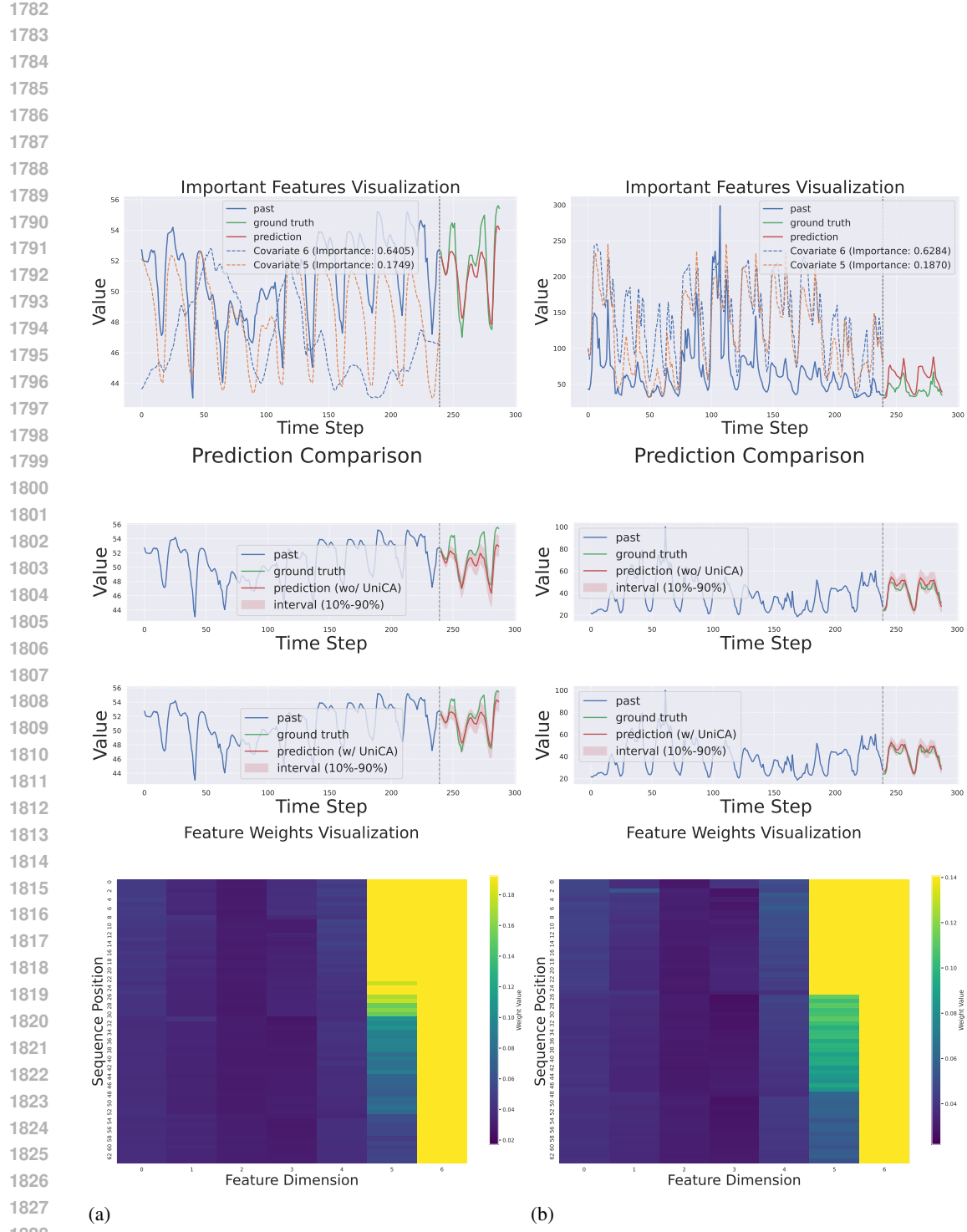
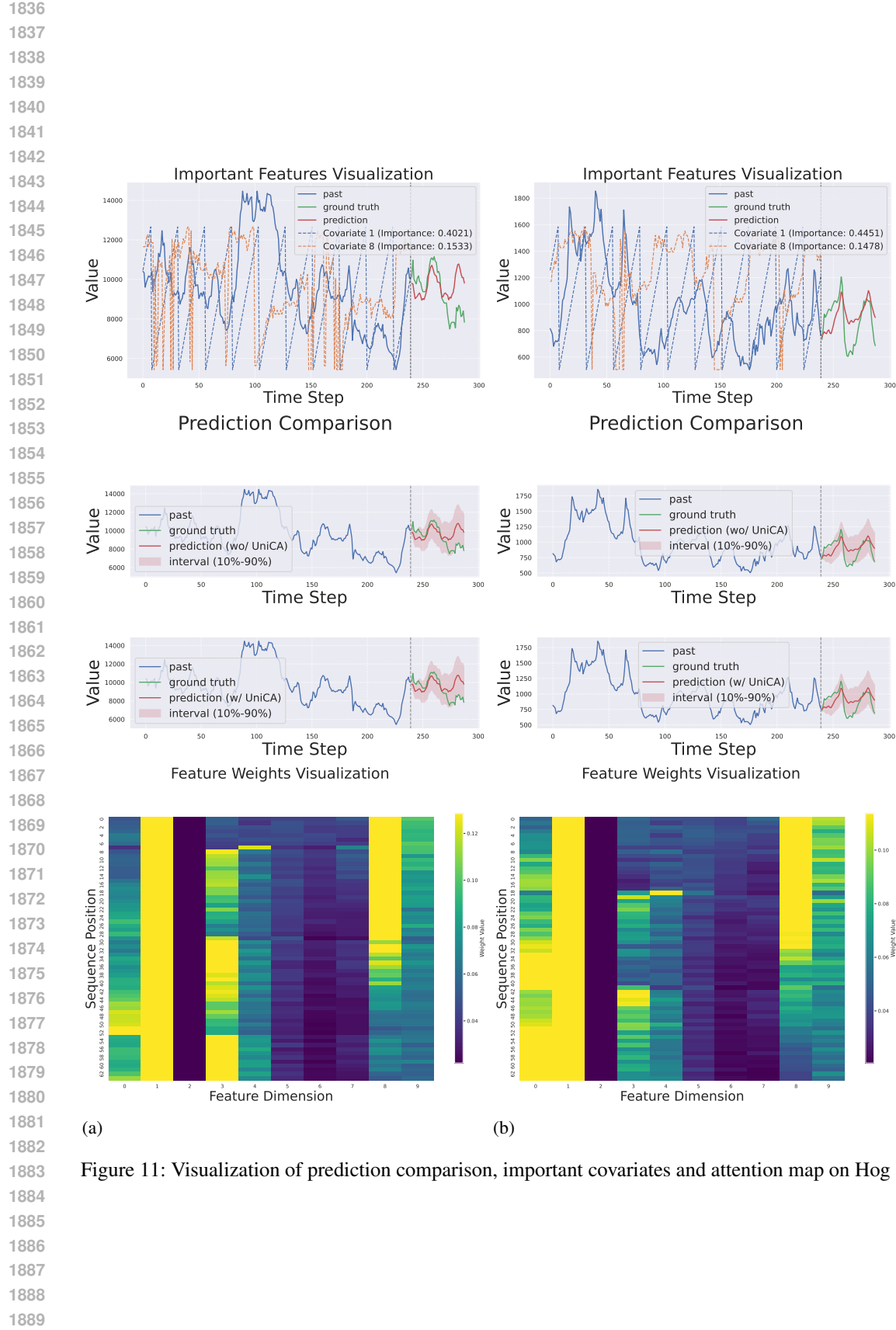


Figure 10: Visualization of prediction comparison, important covariates and attention map on EPF



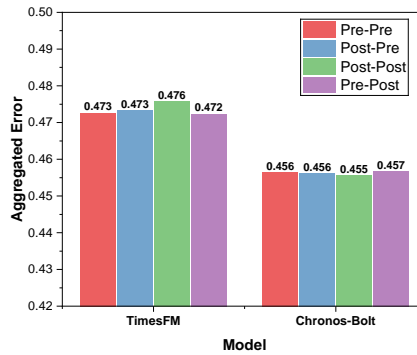


Figure 12: Ablation study on fusion position. Pre-Pre, Post-Pre, Post-Post, and Pre-Post indicate the fusion positions of past and future covariates (before or after the temporal encoder). Results are shown on TimesFM and Chronos-Bolt. Performance remains stable across all configurations, demonstrating the fusion position does not affect the performance much.

(MAE = 0.707) and *SocialGood* (MAE = 0.860) for TimesFM. On the other hand, large language models such as LLAMA do not necessarily outperform smaller encoders. In several cases, GPT and BERT lead to degraded performance in TimesFM, especially for domains with noisier text (e.g., *Environment* and *Security*). The optimal encoder choice appears domain-dependent. For example, in the *Health* domain, GPT yields the best MAE (0.609) under Chronos, while GIST performs best under TimesFM (MAE = 0.692). In the *Security* domain, TimesFM benefits the most from GIST (MAE = 0.707), which is substantially better than other encoders.

These findings suggest that the selection of the modality encoder impacts model performance, depending on the dataset and base model. However, we also warn that the number of observed points in Time-MMD may not be enough to draw a consistent conclusion. This experiment only shows preliminary results.

### G.3 ARCHITECTURE OF COVARIATE HOMOGENIZER

We examine how the architecture of the covariate homogenizer affects forecasting performance in our unified framework. Specifically, we compare two designs: a simple Linear layer and a two-layer MLP, implemented under two different model backbones—Chronos-Bolt and TimesFM, both with UniCA. Results are reported on the MMSP and MMSP<sup>†</sup> benchmarks, as shown in Table 14.

From the results, we observe that for Chronos, the homogenizer design has negligible impact on performance: both Linear and MLP yield nearly identical errors across all metrics. In contrast, TimesFM shows a consistent preference for the Linear homogenizer. For instance, in MMSP, the Average error increases from 0.147 to 0.154 when switching from Linear to MLP, with similar degradation observed in MAE, MSE, and CRPS. This trend holds across both MMSP and MMSP<sup>†</sup>.

These results suggest that more complex homogenizer structures like MLP may introduce unnecessary parameterization and lead to overfitting in already expressive models such as TimesFM, while simpler designs suffice for both backbones. Therefore, we adopt the Linear homogenizer as the default in all main experiments.

### G.4 INFLUENCE OF STATIC COVARIATES

Our UniCA model incorporates the static covariate that most of the datasets do not include. To isolate and quantify the benefit of this feature, we conduct an ablation study on two datasets with static covariates: M5 and Retail<sup>1</sup>. <sup>14</sup> The results, presented in table 15, indicate that incorporating static covariates generally improves performance. The performance gains are most pronounced on the highly diverse Retail dataset, where UniCA improves all metrics for both base models (e.g., reducing the Average metric for TimesFM from 0.672 to 0.655). While on the M5 dataset, the improvements

<sup>14</sup>The M5 dataset includes static covariates ‘item id’, ‘depeartment id’, ‘category id’, ‘store id’, and ‘state id’. The Retail dataset includes ‘city’, ‘state’, ‘type’, ‘cluster’, ‘family’, ‘class’, and ‘perishable’

1944  
1945  
1946  
1947  
1948

1949 Table 13: Forecasting error on Time-MMD subsets with different text encoder.

1950

		Chronos-Bolt (UniCA)				TimesFM (UniCA)			
		GIST	Bert	GPT	LLAMA	GIST	Bert	GPT	LLAMA
Climate	Average	0.507	0.507	0.507	<b>0.507</b>	0.533	0.541	0.542	0.533
	MAE	0.628	0.628	<u>0.628</u>	<b>0.628</b>	0.635	0.630	0.631	0.635
	MAPE	0.421	0.421	0.423	<b>0.421</b>	0.543	0.577	0.578	0.543
	MSE	0.411	0.411	0.411	0.411	0.402	<b>0.401</b>	<u>0.402</u>	0.402
	CRPS	0.568	0.568	0.567	0.567	<b>0.552</b>	0.558	0.556	<u>0.552</u>
Energy	Average	<b>0.879</b>	<u>0.890</u>	0.893	0.903	0.904	0.915	0.907	0.954
	MAE	<b>0.921</b>	0.929	<u>0.928</u>	0.937	0.957	0.972	0.934	0.968
	MAPE	0.831	0.850	0.866	0.876	<b>0.795</b>	<u>0.811</u>	0.925	0.971
	MSE	<b>0.865</b>	0.874	0.871	0.882	0.934	0.935	<u>0.866</u>	0.934
	CRPS	<b>0.899</b>	0.907	0.906	0.916	0.928	0.944	<u>0.903</u>	0.944
Environment	Average	0.625	0.625	0.625	<b>0.625</b>	0.642	1.103	0.661	1.024
	MAE	<u>0.738</u>	0.738	0.738	<b>0.738</b>	0.756	1.181	0.754	1.095
	MAPE	0.666	0.667	0.666	<u>0.666</u>	<b>0.656</b>	1.189	0.716	1.145
	MSE	<u>0.560</u>	0.561	0.560	<b>0.560</b>	0.599	1.114	0.620	0.982
	CRPS	0.536	0.536	<u>0.536</u>	<b>0.536</b>	0.556	0.930	0.554	0.875
Health	Average	0.612	<u>0.609</u>	<b>0.609</b>	0.617	0.692	0.693	0.710	0.709
	MAE	0.697	<b>0.694</b>	0.694	0.702	0.753	0.754	0.769	0.764
	MAPE	<u>0.565</u>	0.569	<b>0.565</b>	0.573	0.684	0.679	0.698	0.718
	MSE	0.484	<b>0.479</b>	<u>0.481</u>	0.490	0.600	0.604	0.623	0.612
	CRPS	0.699	<u>0.696</u>	<b>0.695</b>	0.703	0.733	0.735	0.750	0.742
Security	Average	0.705	0.706	0.702	0.698	<b>0.593</b>	0.663	0.879	<u>0.642</u>
	MAE	0.860	0.862	0.858	0.854	<b>0.707</b>	0.785	1.009	<u>0.762</u>
	MAPE	0.536	0.537	0.532	0.526	<b>0.467</b>	0.553	0.854	<u>0.526</u>
	MSE	0.660	0.660	0.658	0.656	<b>0.578</b>	0.624	0.747	<u>0.613</u>
	CRPS	0.764	0.765	0.761	0.757	<b>0.621</b>	0.689	0.907	0.668
SocialGood	Average	0.790	0.790	0.781	0.790	0.664	<u>0.656</u>	0.661	<b>0.654</b>
	MAE	0.860	0.860	0.834	0.860	0.699	<u>0.689</u>	0.695	<b>0.687</b>
	MAPE	0.666	0.666	0.673	0.666	0.547	<u>0.530</u>	0.541	<b>0.529</b>
	MSE	0.784	0.784	0.791	0.784	0.717	<b>0.711</b>	0.717	<u>0.716</u>
	CRPS	0.850	0.850	0.827	0.850	0.694	0.692	0.690	<b>0.683</b>

1975

1976

1977

1978

1979

1980

1981

1982

1983

1984

1985

1986 Table 14: Forecasting error on MMSP with different designs of covariate homogenizer.

1987

		Chronos-Bolt (UniCA)		TimesFM (UniCA)	
		Linear	MLP	Linear	MLP
MMSP	Average	0.121	<b>0.120</b>	<b>0.147</b>	0.154
	MAE	0.193	<b>0.193</b>	<b>0.229</b>	0.236
	MAPE	0.019	<b>0.019</b>	<b>0.046</b>	0.050
	MSE	0.090	<b>0.090</b>	<b>0.098</b>	0.106
	CRPS	0.180	<b>0.180</b>	<b>0.215</b>	0.222

1993

1994

1995

1996

1997

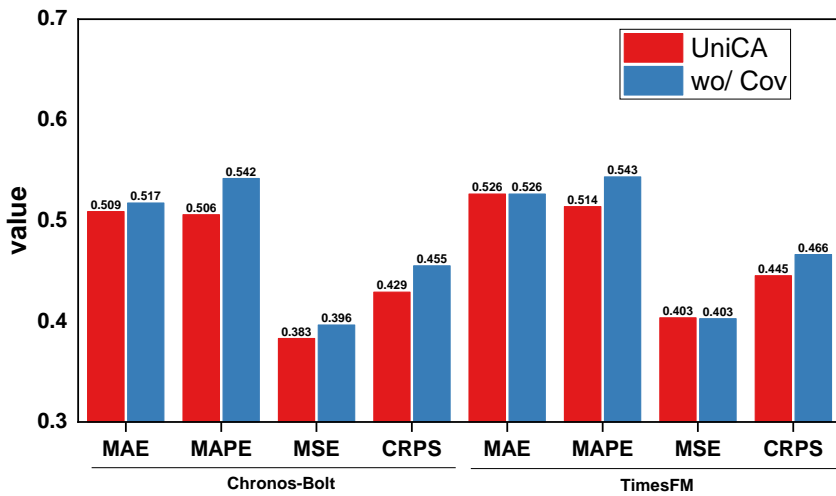


Figure 13: Comparison between the full UniCA model (red) and an ablated version (UniCA w/o Cov, blue) where the covariate adaptation parameters are introduced but the covariate influence is intentionally gated to zero. A lower score is better.

are modest but still noticeable in several metrics (e.g., Chronos-Bolt’s MAPE drops from 0.779 to 0.764, MSE from 0.581 to 0.566). These findings suggest that static variables provide useful categorical and contextual information that enhances model generalization, especially in datasets with diverse item-level characteristics like Retail.

Table 15: Ablation study on the impact of static covariates, conducted on the M5 and Retail datasets. Results show that adding static variables generally improves performance, especially on the Retail dataset, indicating their importance for capturing categorical and contextual information.

Dataset	Metric	Chronos-Bolt		TimesFM	
		wo/ static	w/ static	wo/ static	w/ static
M5	Average	0.625	<b>0.613</b>	<b>0.609</b>	0.613
	MAE	0.706	<b>0.699</b>	<b>0.699</b>	0.701
	MAPE	0.779	<b>0.764</b>	<b>0.731</b>	0.737
	MSE	0.581	<b>0.566</b>	<b>0.581</b>	0.587
	CRPS	0.432	<b>0.424</b>	<b>0.425</b>	0.426
Retail	Average	0.680	<b>0.656</b>	0.672	<b>0.655</b>
	MAE	0.720	<b>0.712</b>	0.712	<b>0.709</b>
	MAPE	0.702	<b>0.655</b>	0.707	<b>0.648</b>
	MSE	0.799	<b>0.769</b>	0.781	<b>0.776</b>
	CRPS	0.499	<b>0.489</b>	0.486	<b>0.485</b>

## G.5 IMPACT OF COVARIATES

To see whether UniCA’s performance gains simply stem from the introduction of additional trainable parameters rather than the effective integration of covariates, we designed a crucial ablation study. We created an ablated model, denoted as UniCA w/o Cov, which retains the exact same model structure and the same number of trainable parameters as the full UniCA model. However, in this ablated version, we intentionally **set the gating mechanism for all covariates to zero throughout the training and inference processes**. This ensures that while the extra parameters are present and trained, the adapted covariate features are prevented from influencing the TSFM backbone. We compare the full UniCA model against this UniCA w/o Cov variant using both Chronos-Bolt and TimesFM backbones across all metrics.

The results of this ablation study are presented in Figure 13. For nearly all metrics and both backbones, the full UniCA model (red bars) significantly outperforms the ablated UniCA w/o Cov model (blue bars). For instance, with the Chronos-Bolt backbone, UniCA achieves 0.509 MAE and 0.383 MSE, substantially better than the w/o Cov model’s 0.517 MAE and 0.396 MSE. A similar

2052 pattern holds for TimesFM, particularly for the MAE and MAPE metrics. The consistent degra-  
 2053 dation in performance for the `w/o Cov` configuration clearly demonstrates that the performance gain  
 2054 is not merely due to the additional parameters introduced by the adaptation layer. Instead, the gains  
 2055 are primarily attributable to the **effective and meaningful integration of external covariate infor-**  
 2056 **mation** enabled by the learned adaptation and gating mechanism, thereby validating the core design  
 2057 of UniCA.

## 2058 G.6 ROBUSTNESS TO NOISY COVARIATES

2061 To verify UniCA’s stability against irrelevant external information, we conducted a robustness ex-  
 2062 periment by introducing a purely noisy covariate to all benchmark datasets. This synthetic feature  
 2063 was generated as white noise, sampled from  $\mathcal{N}(0, 1)$ , and is entirely uninformative and future-  
 2064 unknowable, simulating a low-quality input that a robust model should ignore. The UniCA model  
 2065 in its `w/ Noise` configuration processes this noise alongside any existing covariates. We com-  
 2066 pared the performance of UniCA (`w/ Noise`) against the Zero-Shot (ZS) baseline and the original  
 2067 UniCA configuration, testing both Chronos-Bolt and TimesFM backbones, with the goal of ensuring  
 2068 the adaptation mechanism does not catastrophically integrate non-predictive features.

2069 Table 16: Performance comparison of UniCA and the Zero-Shot (ZS) baseline when UniCA is pro-  
 2070 vided with a purely random, future-unknowable noisy covariate (`w/ Noise`). Results are averaged  
 2071 across all benchmark datasets, demonstrating UniCA’s resilience to irrelevant noise inputs.

	Chronos-Bolt			TimesFM		
	ZS	UniCA	w/ Noise	ZS	UniCA	w/ Noise
<b>Avg</b>	0.472	0.457	0.468	0.473	0.472	0.475
<b>MAE</b>	0.521	0.509	0.518	0.530	0.526	0.526
<b>MAPE</b>	0.522	0.506	0.516	0.523	0.514	0.523
<b>MSE</b>	0.403	0.383	0.397	0.402	0.403	0.403
<b>CRPS</b>	0.441	0.429	0.441	0.437	0.445	0.446

2081 The results, summarized in Table 16, confirm UniCA’s strong resilience to noisy covariates. With  
 2082 the Chronos-Bolt backbone, UniCA (`w/ Noise`) shows only a marginal performance degradation  
 2083 (Avg Metric  $0.457 \rightarrow 0.468$ ) and still outperforms the ZS baseline ( $0.468$  vs  $0.472$ ). This suggests  
 2084 the model’s feature integration module effectively suppresses the disturbance from the pure noise.  
 2085 The stability is even clearer with the TimesFM backbone, where the performance is nearly identical  
 2086 ( $0.472 \rightarrow 0.475$ ). This high degree of stability validates the design of the UniCA architecture: its  
 2087 adaptation layer is highly effective at identifying and mitigating the impact of uninformative or noisy  
 2088 input features, ensuring that the integration of external data does not compromise the model’s core  
 2089 forecasting accuracy.

## 2091 G.7 FUSION ARCHITECTURE

2093 To justify the choice of Gated Residual Network (GRN) and Gated Linear Unit (GLU) for covariate  
 2094 adaptation and fusion, we conducted an ablation study against a simpler alternative. The reviewer  
 2095 questioned the necessity of these specific non-linear structures. We thus implemented a baseline  
 2096 fusion mechanism, termed **Weight Fusion**, where the complex GRN/GLU adaptation module is re-  
 2097 placed by a simple, weight-learnable linear combination (a single fully connected layer followed by  
 2098 a linear output) before fusion with the TSFM backbone’s representations. This alternative maintains  
 2099 a similar parameter count but removes the complex gating and non-linear residual structure. We  
 2100 compare the performance of the full UniCA model against this simpler Weight Fusion approach,  
 2101 as well as the Zero-Shot (ZS) baseline, across all metrics and both Chronos-Bolt and TimesFM  
 2102 backbones.

2103 The results of the fusion mechanism ablation are presented in the table. Across all metrics and  
 2104 both backbones, the full UniCA model consistently achieves the best performance. Specifically, the  
 2105 simple Weight Fusion mechanism performs noticeably worse than the full UniCA model and, in  
 many cases (e.g., Chronos-Bolt Avg: 0.471, TimesFM Avg: 0.478), its performance degrades close

2106 Table 17: Performance comparison between the full UniCA model (using GRN/GLU for adaptation)  
 2107 and an alternative "Weight Fusion" mechanism where the complex adaptation module is replaced  
 2108 by a simple trainable weighted summation. A lower score is better, validating the superiority of the  
 2109 non-linear GRN/GLU structure.

	Chornos-Bolt			TimesFM		
	ZS	UniCA	Weight Fusion	ZS	UniCA	Weight Fusion
<b>Avg</b>	0.472	0.457	0.471	0.473	0.472	0.478
<b>MAE</b>	0.521	0.509	0.519	0.530	0.526	0.532
<b>MAPE</b>	0.522	0.506	0.529	0.523	0.514	0.523
<b>MSE</b>	0.403	0.383	0.396	0.402	0.403	0.408
<b>CRPS</b>	0.441	0.429	0.439	0.437	0.445	0.450

2119  
 2120  
 2121 to or even below the Zero-Shot (ZS) baseline (TimesFM Avg: 0.473). For example, with Chronos-  
 2122 Bolt, UniCA's MAE is 0.509, while Weight Fusion's is 0.519. This significant performance gap  
 2123 strongly validates our architectural choice. The GRN and GLU structures are critical because their  
 2124 **gated, non-linear, and residual design** allows the model to selectively adapt and dynamically weigh  
 2125 the contribution of each covariate feature, which is essential for effective fusion with the general-  
 2126 purpose TSFM representations. Simple linear fusion, in contrast, fails to capture the necessary com-  
 2127 plexities for optimal TSFM adaptation.

## 2128 H CORRELATION ANALYSIS OF HOMOGENIZED COVARIATE EMBEDDINGS

2129 To address the reviewer's concern regarding the interpretability and meaningfulness of the homog-  
 2130 enized covariate embeddings, we conducted an analysis of the feature space. The core idea of homog-  
 2131 enization is to transform the diverse covariate inputs into a unified, rich representation space  
 2132 suitable for fusion with the TSFM's temporal embeddings. To demonstrate that these features cap-  
 2133 ture meaningful temporal structure, we calculated the **Pearson Correlation Coefficient** between the  
 2134 first four dimensions of the final homogenized covariate embedding (just before it enters the TSFM  
 2135 backbone) and the target time series for a diverse set of benchmark datasets.

2136 Table 18: Pearson Correlation of Homogenized Embedding Dimensions with the Target Series. The  
 2137 table presents the Pearson correlation coefficient between the first four dimensions of the homoge-  
 2138 nized embeddings (before fusion) and the corresponding target time series across various datasets.  
 2139 The results show that different embedding dimensions capture distinct and meaningful temporal  
 2140 structure related to the target.

	MMSP	Climate	Energy	Environment	Health	Security	SocialGood	Traffic
Feature 1	-0.149	-0.058	0.068	-0.055	0.033	0.052	0.434	0.271
Feature 2	0.415	0.058	-0.419	-0.001	-0.114	0.063	-0.114	0.127
Feature 3	0.310	-0.117	0.113	0.042	0.087	0.105	0.459	0.289
Feature 4	0.222	0.024	0.224	0.037	-0.023	-0.084	-0.371	-0.104

2150  
 2151 The correlation results are presented in the table. While the absolute value of the correlation varies  
 2152 significantly by dataset and feature dimension, the patterns strongly support our claim that the homog-  
 2153 enized embeddings capture meaningful, yet diverse, temporal structures. For instance, in the  
 2154 **SocialGood** dataset, Feature 3 exhibits a strong positive correlation (0.4593), whereas Feature 4  
 2155 shows a moderate negative correlation (-0.3713), indicating that different dimensions of the embed-  
 2156 ding are learning to capture distinct aspects of the underlying temporal dynamics of the target series.  
 2157 The general non-zero correlations across datasets (e.g., strong correlation in **MMSP** and **Traffic**)  
 2158 confirms that the adaptation process successfully transforms the raw, disparate covariate informa-  
 2159 tion into a fixed-length embedding that is temporally structured and relevant to the forecasting task,  
 which is a necessary condition for effective fusion.

## 2160 I DISCUSSION OF LIMITATION

2161  
2162 UniCA assumes temporal alignment between covariates and the target series, which we approximate  
2163 using imputation and missing-value indicators. However, more effective alignment strategies may  
2164 exist. Additionally, noisy or conflicting covariates can degrade performance. Future work may in-  
2165 incorporate uncertainty-aware fusion, handle non-aligned or partially observed covariates, and embed  
2166 task-specific inductive biases to enhance the robustness and generalizability of TSFM adaptation.

## 2168 J THE USE OF LLMs

2169  
2170 We utilized a Large Language Model (LLM) to assist in the writing process of this paper. The pri-  
2171 mary use of the LLM was for improving the language, style, and readability of the text. This included  
2172 refining sentence structure, correcting grammatical errors, and ensuring consistency in terminology.  
2173 All intellectual contributions, including the research ideas, methodology, and conclusions, are solely  
2174 the work of the human authors. The authors have reviewed and take full responsibility for the entire  
2175 content of this paper, ensuring its originality and scientific accuracy.

2176  
2177  
2178  
2179  
2180  
2181  
2182  
2183  
2184  
2185  
2186  
2187  
2188  
2189  
2190  
2191  
2192  
2193  
2194  
2195  
2196  
2197  
2198  
2199  
2200  
2201  
2202  
2203  
2204  
2205  
2206  
2207  
2208  
2209  
2210  
2211  
2212  
2213